Peer-reviewed version available at *Int. J. Mol. Sci.* **2020**, *21*, 1894; doi:10.3390/ijms21051894

The polymorphic PolyQ tail protein of the Mediator Complex, Med15, regulates variable response to diverse stresses

Jennifer E.G. Gallagher*, Suk Lan Ser, Michael C. Ayers, Casey Nassif, Amaury Pupo

Department of Biology, West Virginia University, 53 Campus Drive, Morgantown WV 26506

*corresponding author

Jennifer Gallagher

53 Campus Drive, LSB 3140

West Virginia University

Morgantown, WV 26506

jegallagher@mail.wvu.edu

Running title: Polymorphic Med15 and stress in yeast

Keywords: Mediator, stress, MCHM, Med15, Snf1, polyQ, protein chaperone, master variator, intrinsically disordered regions, yeast, hydrotrope, transcription factors, Myc tag, inorganic phosphate

Peer-reviewed version available at *Int. J. Mol. Sci.* **2020**, *21*, 1894; doi:10.3390/ijms21051894

Abstract

The Mediator is composed of multiple subunits conserved from yeast to humans and plays a central role in transcription. The tail components are not required for basal transcription but are required for response to different stresses. While some stresses are familiar such as heat, desiccation, and starvation, others are exotic, yet yeast can elicit a successful stress response. MCHM is a hydrotrope that induces growth arrest in yeast. We found that a naturally occurring variation in the Med15 allele, a component of the Mediator tail, altered the stress response to many chemicals in addition to MCHM. Med15 contains two polyglutamine repeats (polyQ) of variable lengths that change the gene expression of diverse pathways. Med15 protein existed in multiple isoforms and its stability was dependent on Ydj1, a protein chaperone. The protein level of the Med15 with longer polyQ tracts was lower and turned over faster than the allele with shorter polyQ repeats. MCHM sensitivity via variation of Med15 was regulated by Snf1 in a Myc tag dependent manner. Tagging Med15 with Myc altered its function in response to stress. Genetic variation in transcriptional regulators magnifies genetic differences in response to environmental changes. These polymorphic control genes are master variators.

Background

Changing the transcriptional landscape is a key step in reorganizing cellular processes in response to stress. RNA polymerase II (pol II) transcription is regulated in a stress-specific manner by multiple post-translational modifications and a host of transcription factors (TFs). These transcription factors do not interact directly with pol II and general transcription factors (GTFs), together called the pre-initiation complex, but through a multi-protein complex called the Mediator. The Mediator itself is composed of four domains: the head, body, tail and kinase domains (Figure 1A). The head interacts with pol II and GTFs while the tail interacts with specific TFs (reviewed [1]). The tail is composed of Med2, Med3 (Pgd1), Med5 (Nut1), Med15 (Gal11) and Med16 (Sin4) and the C-terminal end of Med14 connects the tail with the body of the Mediator complex (Figure 1B, (Tsai *et al.* 2014, 2017; Robinson *et al.* 2015)). The tail is the most diverged between species and binding of TF changes the conformation [5].

Med15 has a curious amino acid sequence (reviewed [6]). Med15 from a common lab strain S288c is 16% glutamines and 11% asparagines. The average Q content is 4% and N content is 5% across eukaryotic proteomes [7]. The proportion of Q/N amino acids is higher than expected based on the distribution of amino acids and thermophilic organisms do not have this category of proteins [7]. There are two polyglutamine (polyQ) tracts separated by a polyQA. These regions along with the N-terminal KIX domain interact with TF through multiple sites termed fuzzy domains, which are intrinsically disordered regions. Med15 makes multiple contacts with Gcn4, an environmental stress response-related TF, including at the polymorphic polyQ repeats and KIX domain [8–12]. Overexpression of Med15 causes protein aggregation, presumably via the polyQ and polyQA regions as this region alone aggregates in response to hydrogen peroxide (Zhu *et al.* 2015). Overexpression of the first polyQ and polyQA of Med15 reduces cell growth in unstressed cells and salt exposed yeast but rescues growth in the presence of rapamycin [13]. Full-length Med15 also forms cytosolic foci in yeast exposed to hydrogen peroxide [13]. The pathogenic effects of polyQ proteins were uncovered when the causative mutation for Huntington's disease was discovered [14]. Huntington's disease causes progressive neurodegeneration in people who inherit a single copy of HTT with the polyQ

Peer-reviewed version available at *Int. J. Mol. Sci.* **2020**, *21*, 1894; doi:10.3390/ijms21051894

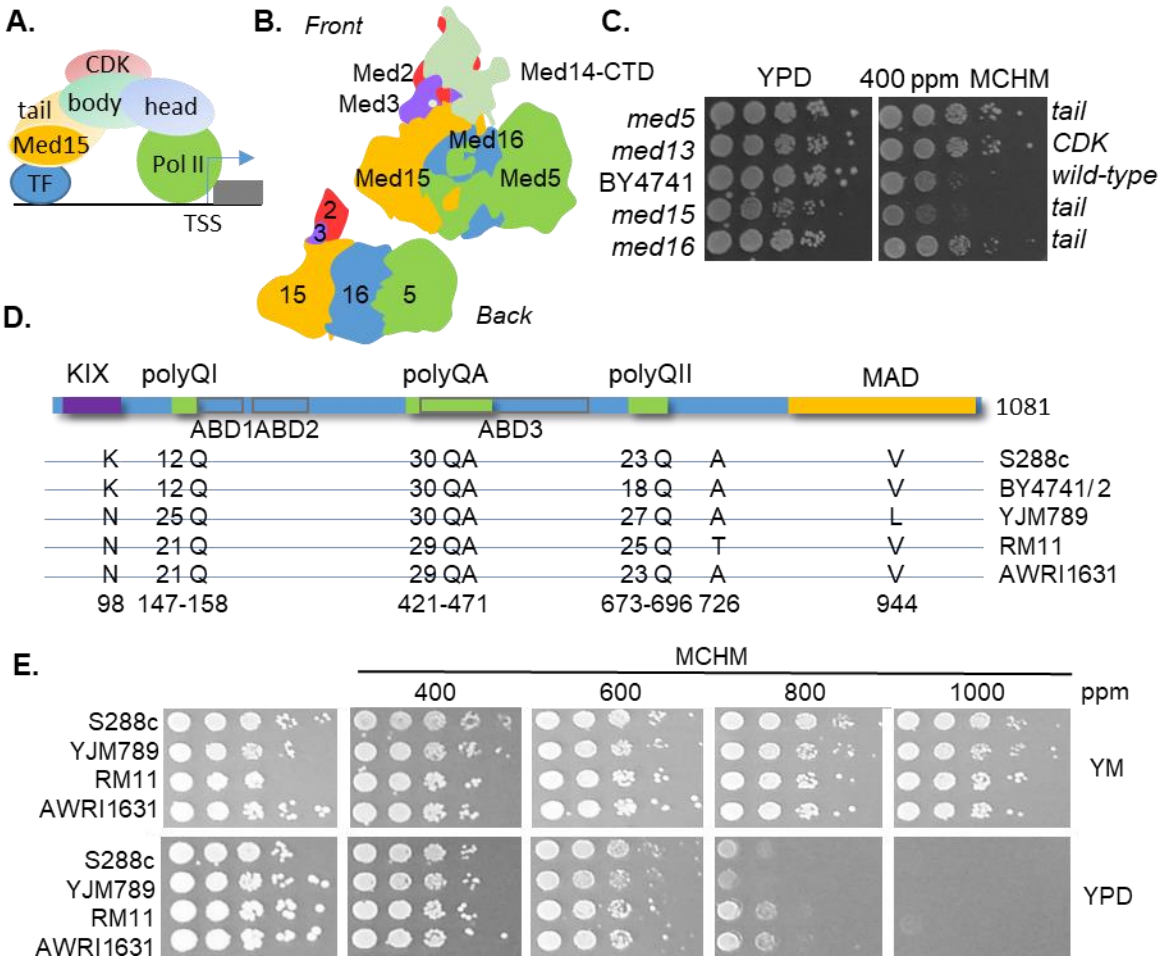

Figure 1 *Role of Mediator tail in response to MCHM* (A) Schematic of the Mediator complex. Med15 as part of the tail subcomplex directly interacts with transcription factors (TF). The body of the Mediator complex tethers the CDK (cyclin-dependent kinase). The head directly interacts with RNA polymerase II (Pol II) at promoter regions to initiate transcription at transcriptional start sites (TSS) of genes (gray box). (B) Representation of protein components of the Mediator tail based on structures and modeling (Robinson *et al.* 2015). Med2 (red), Med14-CTD (light green), Med3 (purple), Med15 (orange), Med16 (blue) and Med5 (green) comprise the tail of the Mediator complex. From the back view, Med5, Med16, Med15, Med3 and Med2 (in order from farthest to closest to the rest of the Mediator complex) associated with Med14 (not pictured here). (C**)** Growth assays of yeast with different components of the Mediator tail knocked out in BY4741 grown with and without 400 ppm MCHM in YPD. (D) Schematic of Med15 protein. Above the blue line are polymorphic domains including the KIX domain, polyglutamine domain I (polyQI), polyglutamine/ alanine domain (polyQA), polyglutamine domain II (polyQII) and the Mediator activation/ association domain (MAD). Under the blue line are the fuzzy domains represented as ABD1-3 (activator-binding domains) in gray outlined boxes (Herbig *et al.* 2010; Brzovic *et al.* 2011). The Med15 polymorphic amino acids are diagramed below from five genetically diverse yeast. Amino acid numbers are based on S288c. (E) Growth assays of genetically diverse yeast strains in the presence of MCHM on different growth media with increasing concentrations of MCHM. Yeast were spotted in ten-fold dilutions onto minimal media supplemented with lysine (YM), or rich media (YPD). RM11, S288c (GSY147), AWRI1631 are MATa prototrophs while YJM789 is a MATalpha *lys2* strain.

expansion inducing protein aggregation (reviewed [15]). Aggregation of polyQ expansion proteins in yeast can be reduced by overexpression of heat shock chaperone proteins [16].

Peer-reviewed version available at *Int. J. Mol. Sci.* **2020**, *21*, 1894; doi:10.3390/ijms21051894

Ydj1 is a highly expressed general type I Hsp40 protein (J-type) chaperone that localizes to the mitochondria, cytoplasm, and nucleus. Yeast lacking Ydj1 function are sensitive to multiple classes of chemicals (Gillies *et al.* 2012). Hsp40 proteins work with Hsp70 to refold misfolded proteins or target them for degradation. They also have roles in translation, translocation across membranes and conformation changes induced by amyloid fibrils. Overexpression of Ydj1 can cure prions (Hines *et al.* 2011). Prions are a group of proteins that not only aggregate but also can induce the aggregation of natively folded proteins. Prions can cause contagious neurodegenerative diseases in humans and switches in the prion state to provide epigenetic plasticity in phenotypic response to stresses by regulating the enzymatic function [19]. When overexpressed, Med15 will aggregate *in vivo* [13]. Overlapping the polyQ domains are the intrinsically disordered regions (IDR) that form fuzzy interactions with TFs, in particular, Gcn4 [8–11]. An N-terminal fragment of Med15 containing the first polyQ and the polyQA domain will form liquid phase condensates, also known as liquid-liquid phase separation, with Gcn4 at low concentrations *in vitro* [20]. These condensates are dynamic and behave like a liquid (reviewed [21]). A mutant of Gcn4 which does not form liquid droplets (phase separation) condensates with Med15, no longer activates transcription [20]. The transition from single phase to liquid phase droplet increases the local concentration of factors by forming non-membrane bound compartments that flow and fuse with surface tension (reviewed in [22]). Liquid phase droplets can be induced by chemicals and act as protein concentrators. IDR interactions may be a more general mechanism to increase the local concentration of proteins within liquid droplets, changing protein conformations, and adding complexity regulating cellular metabolism and environmental responses.

Hydrotropes increase the solubility of organic compounds by inducing liquid phase condensates. Currently, hydrotropes are not considered detergents and detergents function at lower concentrations to solubilize compounds. ATP is a biological active hydrotrope [23–25] and RNA can induce changes in solubility of Whi3 via phase separation [26]. These types of hydrotropes act to concentrate compounds, especially proteins. These molecules induce condensates of proteins that separate these molecules in a liquid phase separate from the rest of soluble molecules in a different liquid phase, also known as liquid-liquid phase transitions (LLPS). In 2014, there was a large spill of MCHM (4-methylcyclohexane methanol), a coal-cleaning chemical, into the Elk River in West Virginia, contaminating the drinking water of 300,000 people [27]. Many of those people suffered from various significant illnesses including mild skin irritation, respiratory and gastrointestinal symptoms [28]. MCHM acts as a hydrotrope *in vitro* and preventing protein aggregations [29]. In contrast to ATP and RNA, MCHM can serve as a model hydrotrope to study the effect of hydrotropes on biological systems. RNA and ATP can be rapidly turned over while MCHM is a cyclic hydrocarbon with saturated bonds that are difficult to break. MCHM is an exotic hydrotrope, and yeast would not have been exposed to MCHM. Exposure to MCHM induced growth inhibition in yeast by changing a wide range of biochemical pathways including ionome [29] and amino acids [30]. The Mediator binds upstream of many genes across pathways, including stress-responsive genes. Numerous studies have explored the role of Med15 via knockouts on microarrays and later RNAseq. Removing the entire coding region not only removes the function of a protein but also alters the structure of complexes containing that protein. Gene knockouts are rarely found in nature, while indels, copy number variation, and SNPs are the most common mutations. By assessing the role of naturally variable protein, the integrity of the Mediator is maintained and the specific function of Med15 can be addressed in response to hydrotropic chemicals, such as MCHM.

Peer-reviewed version available at *Int. J. Mol. Sci.* **2020**, *21*, 1894; doi:10.3390/ijms21051894

AMP kinases regulate ATP levels, and the yeast ortholog is a heterotrimeric complex called SNF1 (reviewed in [31]). In glucose limitation or other stresses, Snf1, the catalytically active kinase in SNF1 complex, is phosphorylated on T210 by Tos3, Eml1, or Sak1, Upstream Activating Kinases (USAKs, reviewed in [31]). The protein phosphatase 1 (PP1) negatively regulates SNF1 by dephosphorylation of Snf1 by Glc7 in the presence of glucose. Reg1 regulates the activity of PP1, and in a *reg1* mutant, SNF1 complex is constitutively active because of the lack of dephosphorylation. Snf1 itself forms liquid droplets in the nuclear vacuole junction (reviewed [32]). Myc, a commonly used epitope tag derived from transcription factor, c-Myc, is phosphorylated by SNF1, the yeast homolog of AMP kinase, *in vitro* (M Schmidt, personal communication) and Snf1 physically associates with the Mediator complex [33]. SNF1 regulates multiple nutrient-sensing pathways and is important for response to numerous and diverse chemicals.

The Mediator is essential for regulating the expression of most RNA pol II transcripts [34]. Med15, a component of the Mediator tail complex directly interacts with various transcription factors and has several known phosphorylations that may regulate its function. In yeast, Med15 regulates Oaf1 (fatty acid level sensor), Pdr1 (a transcription factor that regulates pleiotropic drug response), Ino2 (transcription factor involved in inositol response), and Pho4 (basic helix-loop-helix transcription factor of the Myc-family) to name a few [35]. Pho4 is a regulatory factor involved in phosphate metabolism and activates other phosphate regulatory genes such as *PHO5* under low phosphate conditions [36]. Being part of the Myc-family, the DNA binding domain of Pho4 has sequence similarity with various mammalian transcription factors including Myc, which recognizes the palindromic sequence 5'-CACGTG-3 of basic helix-loop-helix motifs (bHLH) [37]. Chimeras of Pho4-Gal4 in which the bHLH region of the transcription factor was replaced with c-myc remain fully functional [38].

MCHM is an exotic hydrocarbon that changes the solubility and presumably the structure of proteins. The initial goal of this research was to characterize how a single polymorphic protein, Med15, regulates gene expression in response to a hydrotrope. As the altered state of protein conformation/ phase (single verse liquid) are coming to light, the highly variable Med15 was further characterized. Polymorphic transcriptional regulators allow a small genetic variation to have a large impact on phenotypic variation. A single polymorphism of threonine to isoleucine removed a potential phosphorylation site in Yrr1, a transcription factor, which confers 4NQO sensitivity but has the benefit of increased respiration [39,40]. These polymorphic proteins are termed master variators [39]. MCHM is a hydrotrope that increases protein solubility [29], and a truncated version Med15, containing polyQI and polyQA can exist as liquid droplets *in vitro* with TFs [20]. Master variators magnify the effect of genetic variation on phenotypic plasticity. Genetic variation of Med15 regulated cellular response to MCHM, and in the process, we uncovered how a tag of Myc on Med15 altered the function of the Mediator in conjunction with SNF1 to regulate the cellular response to not only MCHM but to other diverse stressors.

Results

The growth of yeast with different components of the Mediator complex knocked out was tested in the response to MCHM (Figure 1C). As the tail directly interacts with the TFs, *med15, med16,* and *med5* knockouts were tested and *med13* from the CDK was chosen because it is on the other side of the complex from the tail. Mutants in *med5, med13,* and *med16* grew better in

Peer-reviewed version available at *Int. J. Mol. Sci.* **2020**, *21*, 1894; doi:10.3390/ijms21051894

response to MCHM than the parental strain, BY4741, while the growth of the *med15* mutant was inhibited after three days of growth. Med15 is a 120 kDa protein with multiple protein domains (Figure 1D). The KIX domain is at the N-terminal domain and interacts with TFs. Two polyQ tracts are separated by a polyQA tract. Between species, the C-terminal end of Med15 is highly divergent and required for the association to the Mediator complex, via the Mediator activation/association domain (MAD). MAD is heavily phosphorylated but the exact roles of these phosphorylations have not been determined (Albuquerque *et al.* 2008; Holt *et al.* 2009; Soulard *et al.* 2010; Swaney *et al.* 2013). Between polyQI and polyQII and partially overlapping with the polyQA tract are three ABD (Activator Binding Domains) regions (Pacheco *et al.* 2018). The ABDs and KIX domain form fuzzy interactions with TFs (Warfield *et al.* 2014; Tuttle *et al.* 2018). The unusual structure of Med15 leads us to investigate whether Med15 from other strains had genetic variation in the polyQ tracts. Med15 from five genetically diverse yeast had between 12 and 25 Qs in the polyQI and between 18 and 27 Qs in polyQII. The polyQA only differed by one less QA repeat in RM11 and AWRI1631 Med15 alleles. There were three other non-synonymous SNPs: K98N, A726T, and V944L using S288c allele numbering. These strains were then tested on increasing concentrations of MCHM in YPD and YM (yeast minimal media with no amino acids, Figure 1E). There was a mild decrease in growth in the strains in YM at the highest concentration of 1000 ppm MCHM, which is the limit of solubility of MCHM in media, but there was no difference detected across these strains. These strains are prototrophs and are more robust than BY4741. Growth was slowed at 800 ppm MCHM in YPD with YJM789 being the most sensitive.

YJM789 and BY4741 were selected for further study because their alleles of Med15 represent the range of variation in polyQ lengths, differences in MCHM resistance and available genetic markers. Reciprocal hemizygosity assays were carried out. *MED15* was knocked out in haploid parent strains and diploids selected. Both the $MED15^{YJM789}/\Delta$ and the $MED15^{BY}/\Delta$ diploids were equally sensitive to MCHM (Figure 2A). However, when compared to the homozygous mutant, the hemizygotes were more sensitive. Suggesting there is no impact of the different alleles of Med15 on MCHM response in the context of a hybrid Mediator complex, but Med15 is important possibly as a gene dosage effect with respect to the stoichiometry of the Mediator complex.

The gene dosage could mask allelic differences in the diploid hemizygotes, so to control for this, *MED15* was swapped in BY4741 and YJM789 haploid knockouts. *MED15* alleles were cloned from yeast which had their *MED15* alleles tagged with Myc at the chromosomal location with the KanR marker. Both alleles were expressed under their endogenous promoters from a single-copy plasmid. We did find that the Myc tag on Med15 increased the sensitivity of yeast to MCHM when comparing the reciprocal hemizygotes to the untagged strains. The growth of Myc-tagged hemizygous mutants was inhibited at 550 ppm while the untagged mutants were inhibited at 650 ppm (Figure S1A, Figure 2A). *MED15* was knocked out in BY4741 and YJM789 and transformed with the two alleles of Med15-Myc with the empty plasmid as the negative control and were grown in YPD or YM (with MSG as the nitrogen source instead of ammonium sulfate to maintain the selection of the KanR plasmid in minimal media with G418). Wildtype BY4741 grew slower than BY4741 carrying $Med15^{S288c}$-Myc in YPD with low levels of MCHM for

Peer-reviewed version available at *Int. J. Mol. Sci.* **2020**, *21*, 1894; doi:10.3390/ijms21051894

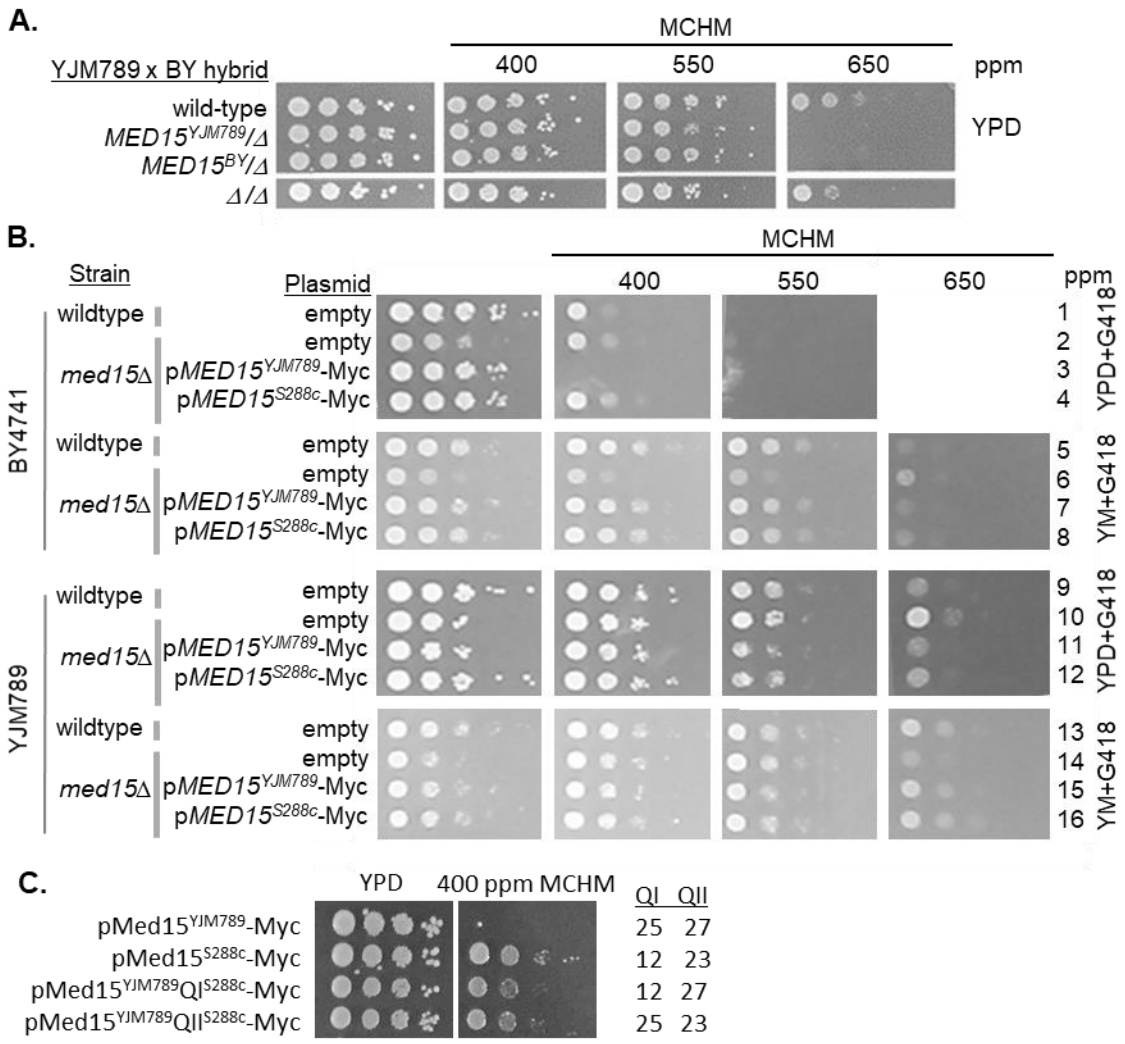

Figure 2 *Genetic variation in Med15 contributes to variation in MCHM response.* (A) Reciprocal hemizygotes of Med15 in BY4741xYJM789 hybrids were grown on MCHM in YPD. Med15 was tagged at the chromosomal locus with 13xMyc at the C-terminal end or knockout with a dominant drug marker in haploid parents. Yeast were then mated, and diploids selected. (B) Med15 allele swap in BY4741 and YJM789 was carried out by cloning Med15-13xMyc with *KanR* onto pRS316. Med15 plasmids were transformed into wildtype and *med15::NatR* stains in the BY4741 and YJM789 (YJM789K5a, a MATa prototroph) backgrounds. Plasmids were maintained by growth on YPD with G418. Glutamate (MSG) was used as the nitrogen source in minimal media with histidine, uracil, leucine, and methionine to supplement BY4741 so that G418 would be selective and maintain the plasmid. The empty plasmid is pGS35 (*KanR*). (C) Growth of BY4741 *med15* mutants expressing polyQI and polyQII domain swaps in Med15^{YJM789}-Myc. The length of each polyQ for each allele is noted to the right of the figure.

two days (Figure 2B row 1 and 4). In these same conditions, there is very little change in the growth of the BY4741 *med15* knockout (Figure 2B row 2). However, the yeast with Med15^{YJM789}-Myc was severely affected by MCHM. Consistent with the growth of the other strains, more MCHM was required in YM to slow growth of yeast and there was no difference between the three alleles of Med15 (row 5, 6, and 8). The *med15* knockout grew slower in YM but appeared to be not affected by MCHM when the slow growth of this mutant was also taken into account

Peer-reviewed version available at *Int. J. Mol. Sci.* **2020**, *21*, 1894; doi:10.3390/ijms21051894

(Figure 2B row 6). YJM789 growth was not affected by the alleles of Med15-Myc expressed in YPD or YM (Figure 2B row 9, 11, 12, 13, 15, 16). YJM789 *med15* mutant grew slower in YM, yet mutant growth was about the same in 400 ppm MCHM in YPD and YM. At 550 and 650 ppm MCHM in YPD, the knockout grew better in YPD than yeast with Med15-Myc but not in YM.

It is surprising that BY4741 Med15^{YJM789}-Myc yeast were more sensitive to MCHM in YPD than the *med15* knockout yeast. To test if the Med15^{YJM789}-Myc was a dominant-negative allele, Med15^{YJM789}-Myc was expressed in wildtype BY4741 with endogenous Med15^{BY}. Expressing both Med15^{YJM789}-Myc and Med15^{BY} in yeast did not change growth in YPD with MCHM and no difference was noted when compared to yeast with Med15^{S288c}-Myc and Med15^{BY} in the BY4741 *med15* knockout (Figure S1B row 7 and 8). However, yeast expressing both Med15^{YJM789}-Myc and Med15^{BY} were more sensitive to MCHM in YM with high levels of MCHM (Figure S1B row 7 and 8). To assess the impact of the variation of each polyQ tract on yeast growth in the presence of MCHM, the polyQ domains from Med15^{S288c} were used to replace the respective domains in Med15^{YJM789}. Both polyQ^{S288c} swapped alleles improved the growth of the yeast containing Med15^{YJM789} (Figure 2C). Although, each polyQ^{S288c} swap partially rescued the growth defect contributed by the Med15^{YJM789} allele. We continued studies with Med15^{YJM789} and Med15^{S288c} for comparison.

To determine if the protein levels of Med15 contribute to differences in MCHM sensitivity, protein levels of the cloned alleles Med15-Myc in the allele swapped strains were measured. Med15-Myc proteins were immunoprecipitated because the levels are too low to detect by western blot without enrichment. Yeast were grown to mid-log phase in YPD or YM with

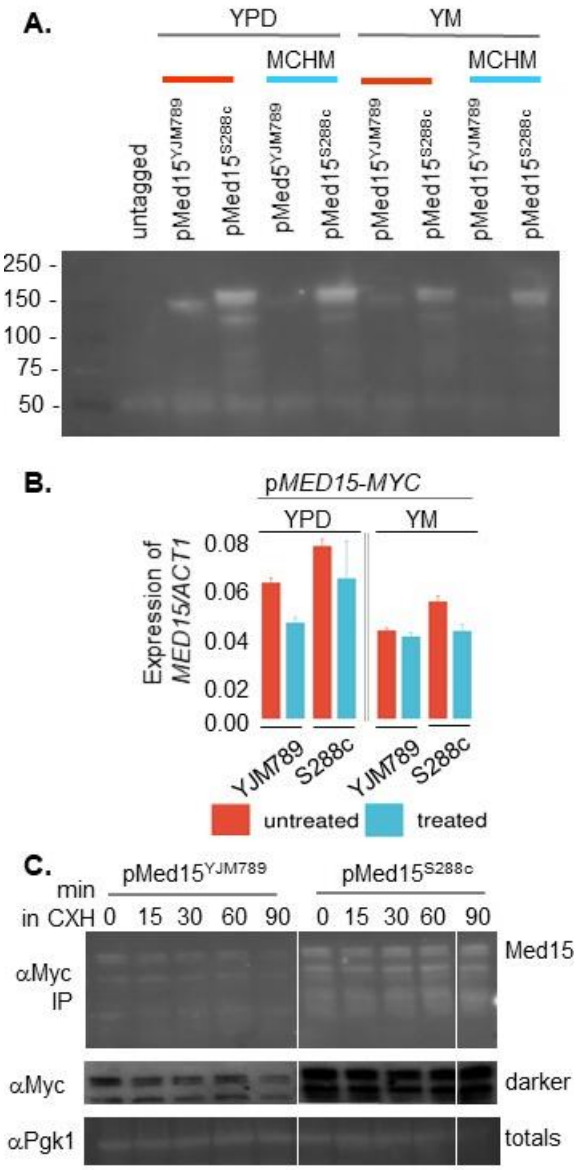

Figure 3 *Changes in the gene expression levels of different alleles of Med15 treated with MCHM*. (A) Protein levels of Med15-13xMyc expressed from a plasmid in BY4741 *med15* yeast. Yeast were grown in selective media until mid-log and then shifted to 550 ppm MCHM for 90 minutes. Med15-13xMyc was immunoprecipitated from equal amounts of protein extract. (B) mRNA levels of *MED15* expressed from a plasmid in BY4741 *med15* yeast normalized to *ACT1* mRNA. Transcript levels were extracted from RNAseq data. Yeast were grown in YPD (with G418) or YM (yeast minimal media supplemented with HLM) and then treated with 550 ppm MCHM for 30 minutes. (C) Western blot of Med15-Myc immunoprecipitated from BY4741 carrying YJM789 and S288c alleles of Med15 from yeast grown in YPD at 0, 15, 30, and 90 minutes after the addition of cycloheximide. The total lysate was run separately and Pgk1 was blotted as a loading control.

Peer-reviewed version available at *Int. J. Mol. Sci.* **2020**, *21*, 1894; doi:10.3390/ijms21051894

amino acids supplemented and then shifted to media containing MCHM for 30 minutes. Med15^{YJM789}-Myc levels were lower than Med15^{S288c}-Myc in all conditions tested, YPD, YM, and with and without MCHM. In general, the levels of both alleles were lower in YM. Med15^{YJM789}-Myc levels also appeared to decrease in YPD with MCHM but the decreased levels did not explain the MCHM sensitivity as the *med15* knockout was not as sensitive as yeast carrying the Med15^{YJM789}-Myc allele. Similarly, yeast with Med15^{YJM789}-Myc grew similarly to yeast carrying Med15^{S288c}-Myc in YM and the levels of Med15 protein were very different in YM (Figure 3A). It is also curious to note, with the Myc tagged Med15^{S288c} is predicted to be 140 kDa with pI at 6.61 and Med15^{YJM789} is predicted to be 142 kDa with a pI at 6.48. Med15^{S288c}-Myc protein runs above the 150 kDa marker as multiple bands despite being shorter than Med15^{YJM789}-Myc which runs truer to size. In part, the differences in Med15 protein levels could be attributed to differences in mRNA levels. Global mRNA levels were quantified by Illumina sequencing of three biological replicates (Figure 3B). *MED15^{YJM789}*-Myc mRNA decreased in YPD with MCHM and was equivalent in YM irrespective of MCHM. The levels of *MED15^{S288c}*-Myc mRNA levels also tracked with protein levels. The *MED15* promoter contains 4 SNPs that were included on the plasmid which are in relation to the start codon of S288c to YJM789: A-8T, A-209G, A-365G, and T-449C. Next, the stability of the Med15 proteins was measured by treatment with cycloheximide, which blocks translation. While Med15^{YJM789}-Myc protein levels were lower than Med15^{S288c}-Myc by the end of the time course, Med15^{YJM789} had decreased more relative to the levels of Med15^{S288c} (Figure 3C)..

Med15 is important for response to many different stresses and to determine which genes were differentially regulated RNAseq was carried out. BY4741 and its isogenic *med15* knockout were grown to log-phase and then treated with MCHM. In YPD, 149 genes were upregulated, and 184 genes were downregulated in the *med15* knockout compared to BY4741 (Figure 4A and Table S1). The downregulated genes were related to metabolic processes of nucleosides and ribonucleosides, pyruvate metabolism, carbohydrates, and organophosphates catabolism, small molecule biosynthesis, oxidoreduction coenzyme metabolism, among others (Figure S2). In part downregulation of these metabolic genes in absence of the Med15 protein may explain the reduced growth of the knockouts in rich media or regulation of these genes were dependent on Med15, then downregulation would slow the growth. Other conditions that reduce growth such as petite yeast [29] or treatment with chemicals that reduce growth [40], demonstrate downregulation of similar pathways. In YPD, 46 GO terms were upregulated and 76 were downregulated, while in YM, 35 were upregulated and 72 were downregulated. This set was not enriched in genes related to heat-shock response, drug/ toxin transport, stress response, and cellular import as in [45] or in ribosome biogenesis as in [35]. Sporulation related genes were upregulated (Figure S3), as previously reported in [45,46]; although, they are not yet known to have functional relevance in haploid cells. There were also genes involved in cell development, reproduction, morphogenesis and sulfur compound biosynthetic process. Previously a study found that genes were upregulated for sulfur metabolism in the *med15* mutant [45].

When MCHM was added, the number of differentially expressed genes increased in the *med15* mutants. There were 468 genes upregulated and 278 downregulated (Figure 4B and Table S1). There was extensive overlap in metabolic pathways in the downregulated genes in the *med15* knockout compared to BY4741 in YPD only and YPD + MCHM, with only three more GO terms appearing: monosaccharide metabolism and organic acid and carboxylic acid biosynthesis

Peer-reviewed version available at *Int. J. Mol. Sci.* **2020**, *21*, 1894; doi:10.3390/ijms21051894

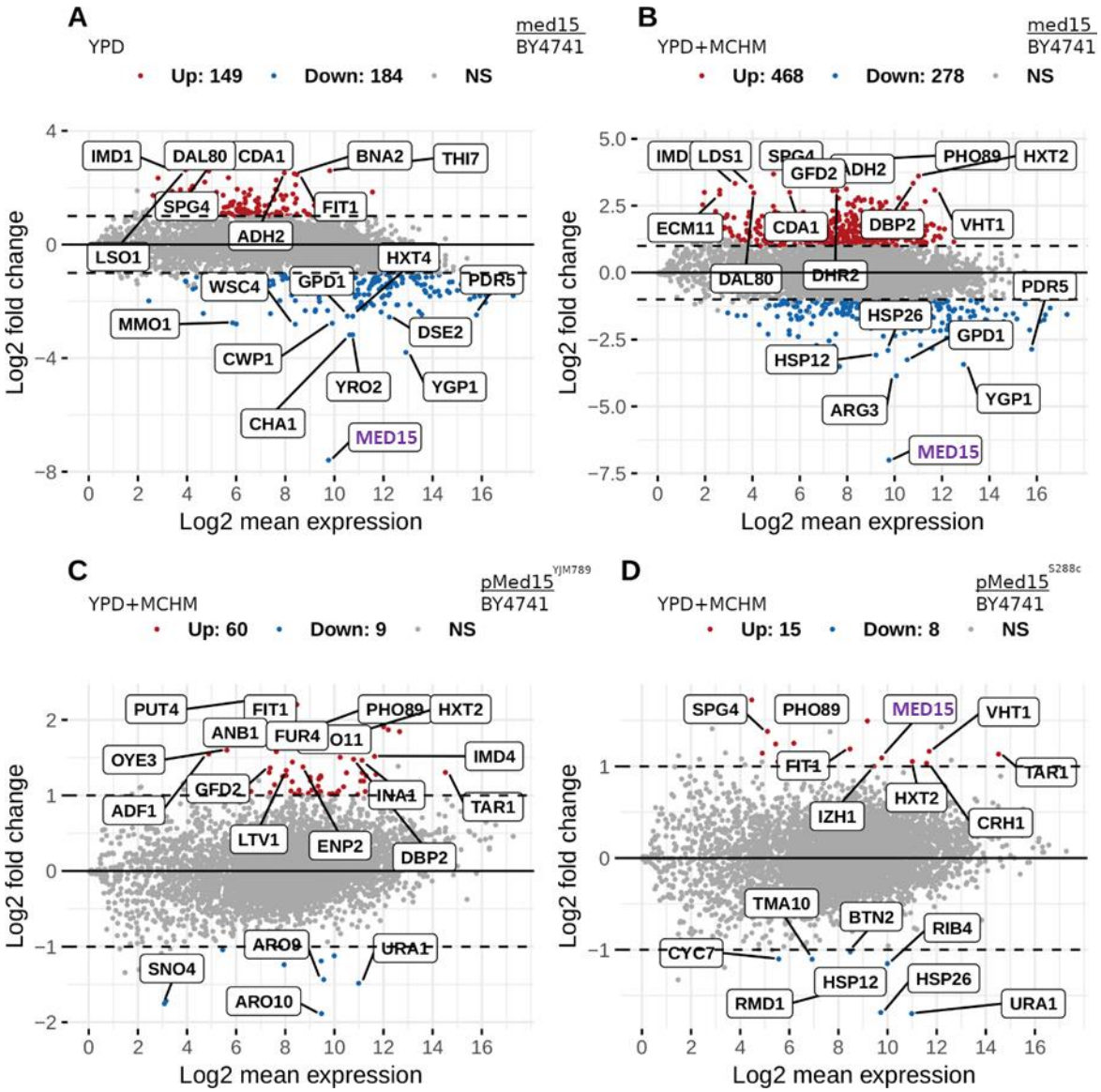

Figure 4 Changes in the transcriptome of BY4741 yeast carrying different alleles of Med15 treated with MCHM grown in YPD. (A) Differentially expressed mRNA from wildtype yeast (BY4741) compared to a *med15* knockout strain grown in YPD. (B) Differentially expressed mRNA from wildtype yeast (BY4741) compared to a *med15* knockout strain grown in YPD then shifted to 400 ppm MCHM for 30 minutes displayed on a log scale. (C) Differentially expressed mRNA from wildtype yeast (BY4741) compared to a *med15* knockout strain carrying $Med15^{YJM789}$ expressed from a plasmid grown in YPD then shifted to 550 ppm MCHM for 30 minutes. (D) Differentially expressed mRNA from wildtype yeast (BY4741) compared to a *med15* knockout strain carrying $Med15^{S288c}$ expressed from a plasmid grown in YPD with G418 then shifted to 550 ppm MCHM for 30 minutes.

(Figure S2). The difference was significant in the upregulated genes, not only in the number but in their functionality, as the GO terms overlap was low and a wide set of new terms related to ribosomes, polyamine transport and RNA export from the nucleus appears. It is of note that in our study, *med15* deletion caused the upregulation of ribosome biogenesis genes, contrary to the downregulation observed in [35]. Also, their observed downregulation of this set of genes

Peer-reviewed version available at *Int. J. Mol. Sci.* **2020**, *21*, 1894; doi:10.3390/ijms21051894

was the same in wildtype versus *med15* under osmotic stress, while we only observe the upregulation in the presence of MCHM, suggesting a fundamentally different mechanism of responding to osmotic stress and MCHM induced stress in yeast.

By directly comparing the Med15^{YJM789}-Myc and Med15^{S288c}-Myc effect on gene expression, Med15^{YJM789}-Myc changed the expression of 69 genes and Med15^{S288c}-Myc 23 genes compared to BY4741 when treated with MCHM in YPD (Figure 4 C and D, respectively, Table S1). The functional impact may be minimal as no term came out of the GO analysis (Figure S2 and S3). Eight out of the nine downregulated genes in Med15^{YJM789}-Myc vs BY4741 were involved in small molecule biosynthetic process (Figure S2). Besides ribosome biogenesis, there were upregulated genes related to rRNA processing, ribonucleoside and glycosyl compound biosynthetic processes and ion transport (Figure S3).

The change of the media (YM instead of YPD) provoked a significant change in gene expression variation among the different cases being compared (Figure S4 and Table S1). But, the functional analysis of downregulated genes was strikingly similar to that of yeast grown in YPD (Figure S3 and S6). The functional analysis of upregulated genes in YM showed a different picture, with *med15* knockout versus BY4741. GO terms were almost the same regardless of the presence of MCHM, but three new GO terms appeared in *MED15^{YJM789}-Myc* versus BY4741: sulfate assimilation, cysteine biosynthesis, and secondary metabolism.

Med15 binds upstream of many genes (Dunn, Gallagher, and Snyder, unpublished). Three genes were chosen for further characterization, *PTR2, PUT4,* and *YDJ1.* Ptr2 is a dipeptide transporter [47] and Put4 is the high-affinity proline permease [48]. Nitrogen catabolite repression downregulates transporters and permeases of nonpreferred nitrogen sources when preferred nitrogen sources such as ammonium or glutamine (MSG) are available (reviewed in [49]). At the cell membrane, both of these proteins are downregulated via endocytosis when shifted to a preferred carbon source, with Put4 degradation being faster than Ptr2 [50]. Except in MCHM treatment in YM, the levels of *PTR2* were significantly decreased and the levels of *PUT4* significantly increased in Med15^{YJM789} with

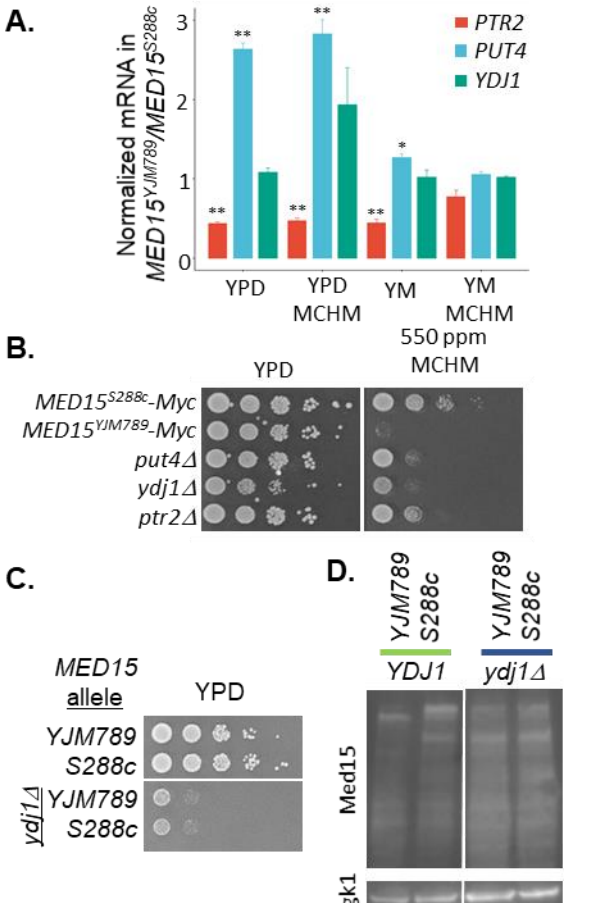

Figure 5 *Conditions that affect the stability of Med15.* (A) Expression levels of *PTR2, PUT4,* and *YDJ1* extracted from RNAseq data from supplemental table ST1 (B) Plasmids containing Med15^{YJM789}-Myc and Med15^{S288c}-Myc were transformed into single mutants of *med15.* The *put4, ptr2,* and *ydj1* in the BY4741 background were grown and serial dilutions of yeast on YPD were grown for 2 days at 30^{o}C and then photographed. (C) Serial dilution of yeast knockouts of *ydj1* yeast expressing YJM789 or S288c alleles of Med15-Myc on YPD. (D) Western blot of YJM789 or S288c alleles of Med15-Myc immunoprecipitated from BY4741 or the *ydj1* mutant which were grown in YPD.

Peer-reviewed version available at *Int. J. Mol. Sci.* **2020**, *21*, 1894; doi:10.3390/ijms21051894

respect to Med15^{S288c} in all other conditions, while the levels of *YDJ1* expression remained the same (Figure 5A). The knockouts of these genes conferred MCHM sensitivity in YPD. However, in YM, only the *ydj1* yeast strain was also sensitive to MCHM (Figure 5B). The role of Ydj1, a protein chaperone, on Med15 function was further characterized. MCHM acts as a hydrotrope that alters protein solubility which is related to protein conformation. Swapping the Med15 alleles in the *ydj1* knockout had no effect on growth. The *ydj1* knockouts were slow-growing in BY4741 (Figure 5B and C) and *ydj1* is lethal in W303 (Caplan and Douglas 1991). The impact of the loss of Ydj1 on Med15 protein levels was measured by western blot (Figure 5D). The Myc tagged protein isoforms were more heterogeneous in size in the *ydj1* mutant and the levels of Med15^{YJM789} increased to match that of Med15^{S288c}. The slowest migrating band of Med15^{YJM789} increased to match that of Med15^{S288c}.

Med15 contains multiple phosphorylations with the C-terminal MAD. It is unknown if these phosphorylations are regulated in a stress-dependent manner. Both alleles of Med15-Myc run as multiple bands that did not appear to change in MCHM treatment (Figure 3A). To determine if other stressors could alter the isoforms of Med15, expressing Med15^{S288c}-Myc were treated with either MCHM or hydrogen peroxide over a 90-minute time course. There was no visible change in the pattern of Myc-tagged proteins in the western blot (Figure S7A). While the effects of MCHM on yeast clearly point to an increase in ROS stress for the cell, wildtype cells seem to be robust enough, on average, to limit this stress, while mutants in certain pathways cannot. To test this hypothesis, we also performed the DHE assay on *med15* mutants (Figure S7B). The endogenous levels of ROS were higher in *med15* and when treated with hydrogen peroxide increased ROS compared to BY4741. The wildtype and mutant strains showed a similar pattern of DHE fluorescence when treated with MCHM, with the appearance of a high ROS population peak that was less intense and broader than hydrogen peroxide. The major difference from the wildtype was an increase in the size of the high ROS population peak. Therefore, *med15* mutants may have an innate sensitivity to MCHM due to their inability to maintain ROS homeostasis.

The growth analysis, protein levels, and transcriptomics of the Med15 allele swaps were carried out with Myc tagged alleles (Figures 2-5). Numerous studies have used these epitope tags and on occasion have noticed negative effects on the function of the protein. The typical control is testing the growth of yeast. Strains carrying either of the Myc tagged alleles experienced growth indistinguishable from untagged alleles on YPD and YM in BY4741 and YJM789 (Figure 2B). However, we began to question this pattern, at least in some stress conditions, upon deeper analysis of the RNAseq (Figure 4D and S4D). Med15 was among the overexpressed genes in Med15^{S288c}-Myc vs BY4741 (log2FC ~1.1) in MCHM treatment and 22 other genes also changed expression (Figure 4D). There was no statistical difference in expression levels of the tagged allele in untreated YPD or YM (Figure S8A and B). Yeast expressing Med15^{S288c}-Myc showed a few genes upregulated in both YPD and YM, such as *PUT4 and PHO89.* Genes that were downregulated encode protein chaperones: *HSP30, HSP4,* and *SSA4* (Figure S8A and B). Initial experiments were carried out in the prototrophic S288c (GSY147) to compare to YJM789 (data not shown) and the Med15^{S288c}-Myc cloned was from genomically tagged GSY147 and YJM789 and inserted into pRS316. However, to take advantage of the Yeast Knockout Collection and study allele effects in a single genetic background, subsequent experiments, including RNAseq, were carried out in BY4741. Med15 polyQII from GSY147 contains 23 glutamines, while BY4741 has 18 glutamines (Figure 1D). We can compare the impact of shorter polyQ tracts in Med15 by comparing RNAseq from yeast carrying p*MED15*^{S288c}-Myc to

Peer-reviewed version available at Int. J. Mol. Sci. 2020, 21, 1894; doi:10.3390/ijms21051894

BY4741. Genes such as *PHO89, PUT4, SSA4, HSP30, URA1,* and *MDH2* were differentially expressed in both YPD and YM (Figure S8A and B). All strains tolerated MCHM better in YM compared to YPD [29] and intracellular levels of metals and other ions increase in MCHM, including phosphate which doubles in YPD with MCHM treatment [29]. Knockouts of *pho89* and a related phosphate transporter, *pho84* were grown in the presence of MCHM. Despite *PHO89* expression increasing in RNAseq, the knockout grew the same as BY4741 and the *pho84* mutant was sensitive to MCHM in YPD and YM (Figure S8C). *PHO89* expression was higher in *med15* knockouts in all conditions tested (Figure 4A, 4B, S4A and S4B), and we conclude that Med15 negatively regulates expression of *PHO89* independent of MCHM. In the RNAseq, the presence of the Myc tag was not taken into account.

Between Med15^{S288c} and Med15^{BY}, only polyQII differed (18 versus 23Q). To explore whether the variation in the polyQII or the presence of the Myc tag was affecting MCHM response, Med15 was tagged at its genomic location in BY4741 and compared to BY4741 carrying Med15^{S288c} with and without the Myc tag. Yeast with Med15^{S288c} without the Myc tag grew slower than yeast carrying Med15^{S288c}-Myc. The presence of the Myc tag on Med15^{BY} slightly increased the MCHM tolerance relative to Med15^{BY} but not as much as yeast with Med15^{S288c}-Myc (Figure S8D). However, these differences were only seen at a lower concentration of 350 ppm MCHM at day 2 compared to concentrations used for RNAseq or initial screening for three days of growth (Figure 6A). The effect of the Myc tag on Med15 was directly tested by cloning endogenous Med15^{YJM789} without the Myc tag and testing growth of yeast on MCHM. The difference in MCHM sensitivity was lost when the Myc tag was absent (Figure 6A). In a genomic screen of the knockout collection for MCHM sensitive mutants, both *snf1* and *reg1* mutants were

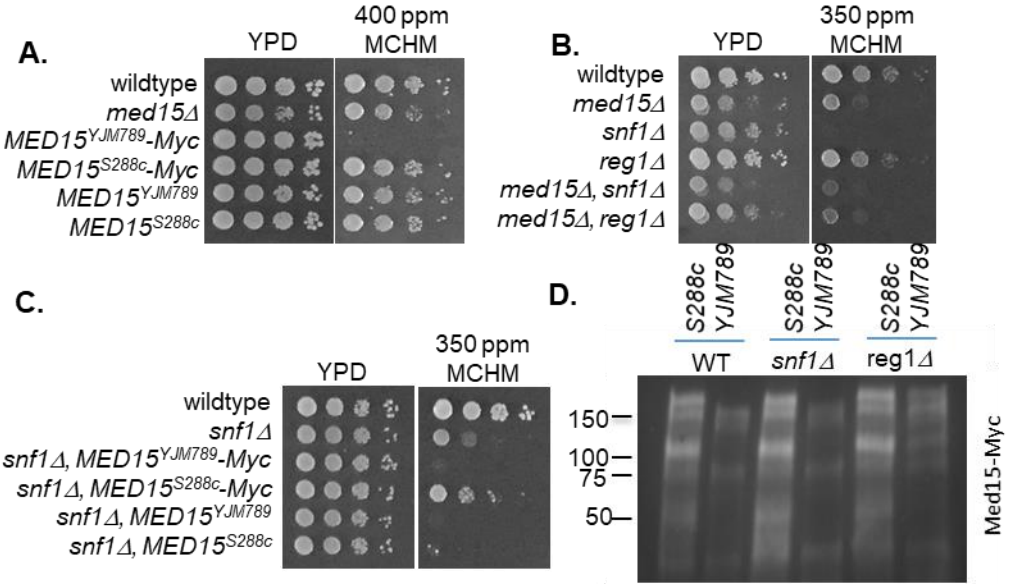

Figure 6 *Impact of Snf1 and Reg1 on yeast expressing different Med15 alleles*. (A) Serial dilutions of BY4741 with different alleles of Med15 that are untagged or C-terminally tagged with 13xMyc grown on YPD or 400 ppm of MCHM and photographed after three days of growth. (B) Serial dilution of BY4741 with single and double mutants containing *med15, snf1,* and *reg1* knockouts grown on YPD or 350 ppm of MCHM. Plates were photographed after two days of growth. (C) Serial dilutions of BY4741 *snf1* mutants expressing different alleles of Med15 with and without the 13xMyc tag grown on YPD or 350 ppm of MCHM. Plates were photographed after three days of growth. (D) Western blot of YJM789 or S288c alleles of Med15-Myc immunoprecipitated from BY4741 grown in YPD with *SNF1* or *REG1* deleted.

Peer-reviewed version available at *Int. J. Mol. Sci.* **2020**, *21*, 1894; doi:10.3390/ijms21051894

identified (Ayers *et al.,* in preparation). Myc is likely phosphorylated by Snf1 *in vitro* (Martin Schmidt, personal communication). Reg1 is the regulator subunit the phosphatase that dephosphorylates Snf1 at T210 which downregulates its kinase activity. In a *reg1* mutant, the SNF1 complex has more kinase activity (reviewed in [31]). *snf1* mutants grow slightly slower than wildtype on YPD and are more sensitive than the *med15* mutant to MCHM while *reg1* mutants grew only a little slower (Figure 6B). The *snf1, med15* double mutant growth was between the two single mutants and the *reg1, med15* double mutant was closer to the *med15* single mutant. In *snf1* mutants, the allele of Med15 expressed had no impact on growth in MCHM, except Med15^{S288c}-Myc (Figure 6C). The pattern of Med15 bands in *snf1* and *reg1* mutants was measured on a western blot. Both Med15 alleles were similar in the wildtype and *snf1* mutant, but Med15^{YJM789}-Myc shifted up and became more similar to Med15^{S288c}-Myc in the *reg1* mutant (Figure 6D).

The two alleles of Med15-Myc conferred different phenotypes not only against MHCM but also other chemicals (Figure 7A). Yeast were grown in an automatic plate reader and the growth difference maximum between alleles during log-phase was plotted. Yeast with Med15^{YJM789}-Myc had greater resistance against compounds that generate free radicals directly, such as hydrogen peroxide and 4NQO, which generates free radicals as it is metabolized (Rong-Mullins *et al.* 2018). MCHM is a volatile compound (Gallagher *et al.* 2015), and when quantitative growth assays were carried out in small volumes, the MCHM evaporates before the end of the growth assay, so growth was only marginally slower in yeast with Med15^{YJM789}-Myc. The Med15^{S288c}-Myc allele conferred resistance to reducing agents that cause unfolded protein response such as beta-mercaptoethanol and DTT, and to DNA damaging chemicals such as camptothecin, and to hygromycin which inhibits translation. Yeast with Med15^{S288c}-Myc were also more resistant to caffeine, which in part can mimic the effects of TOR inactivation, but not to rapamycin which also inhibits TOR. Other chemicals that did not differentially inhibit yeast with different Med15 alleles were Credit41 (glyphosate-based herbicide) which inhibits aromatic amino acid biosynthesis and hydroxyurea which arrests cells in S phase by depleting nucleotides. From this panel of 13 chemicals, 7 were chosen for further characterization in yeast with different alleles of Med15 with and without the Myc tag (Figure 7B). The Myc tag at times flipped the preference of the allele and at other times exaggerated the differences. Only in the presence of caffeine and hygromycin was no difference in growth seen between the untagged alleles, yet increased growth seen of the yeast carrying the Med15^{S288c}-Myc allele. In calcofluor white, the Med15^{S288c}-Myc yeast grew better and in camptothecin, yeast with Med15^{S288c}-Myc grew better while the untagged Med15^{S288c} was marginally better than Med15^{YJM789} for both chemicals.

To assess the impact of the loss of Snf1 and Reg1, quantitative growth assays were conducted in allele swaps with *snf1* and *reg1* mutants. *snf1* mutants with untagged Med15^{S288c} had slightly improved growth compared to *snf1* Med15^{YJM789} in many conditions including in YPD but was not as much as wildtype yeast with the same allele (Figure 7C). In contrast, Med15^{YJM789}-Myc containing *snf1* yeast, grew better in 4NQO, calcofluor white, caffeine, DTT, and hygromycin. Hydrogen peroxide and 4NQO both produce ROS but by different mechanisms. Hydrogen peroxide is directly converted to ROS and 4NQO is converted through a respiration-dependent mechanism [40]. *snf1* yeast with Med15^{S288c}-Myc allele grew better in hydrogen peroxide than wild type yeast with Med15^{S288c}-Myc. Loss of Reg1 had a similar trend in the changes of growth with the notable exception of 4NQO. In that case, the *reg1* Med15^{S288c}-Myc grew better than wildtype (Figure 7D).

Peer-reviewed version available at *Int. J. Mol. Sci.* **2020**, *21*, 1894; doi:10.3390/ijms21051894

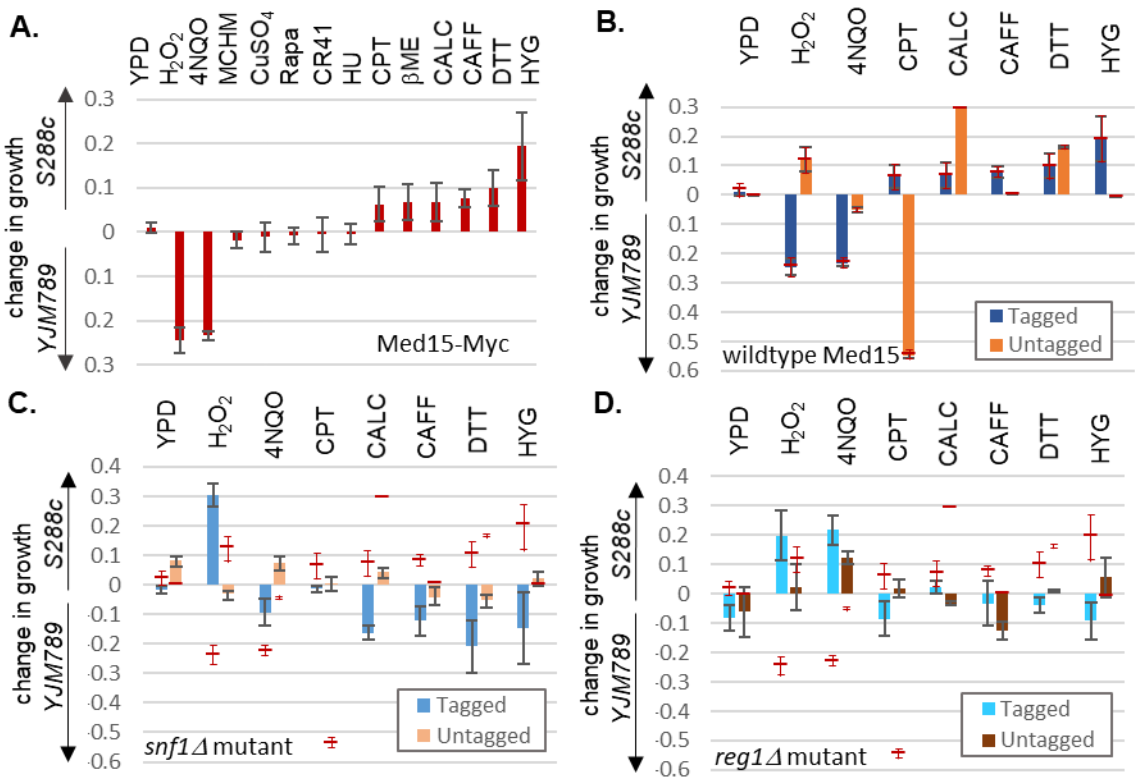

Figure 7 *Quantitative growth assays of BY4741 med15 carrying different alleles of Med15 in snf1 and reg1 mutants with different drugs.* At the time when there was the maximum growth difference, the OD_{600} of yeast carrying $Med15^{S288c}$ was subtracted from OD_{600} of yeast carrying $Med15^{YJM789}$. Values above the y-axis indicate increased growth yeast with the $Med15^{S882c}$ and values below the y-axis indicate that yeast with $Med15^{YJM789}$ grew better than yeast with the other allele. The following chemicals were added: hydrogen peroxide (H_20_2), 4-Nitroquinoline 1-oxide (4NQO), 4-Methylcyclohexanol (MCHM), copper sulfate ($CuSO_4$), rapamycin (Rapa), glyphosate (CR41), hydroxyurea (HU), beta-mercaptoethanol (βME), calcofluor white (CALC), caffeine (CAFF), dithiothreitol (DTT), and hygromycin (HYG). (A) Growth of BY4741 *med15* yeast carrying different alleles of Med15-Myc. (B) Growth of BY4741 *med15* yeast carrying different alleles of Med15 (untagged, blue) or Med15-Myc (tagged, orange). (C) Growth of BY4741 *med15* and *snf1* yeast carrying different alleles of Med15 (untagged, light blue) or Med15-13xMyc (tagged, light orange). The respective values of wildtype yeast from panel B are shown as a thin red line with the standard deviation range is shown as thin red lines. (D) Growth of BY4741 *med15* and *reg1* yeast carrying different alleles of Med15 (untagged, cyan) or Med15-Myc (tagged, brown). The respective values of wildtype yeast from panel B are shown as a thin red line with the standard deviation range is shown as thin red lines.

Discussion

Expansion of polyQ in proteins was discovered to be the cause of numerous neurodegenerative diseases. Slippage of the DNA polymerase during DNA replication and unequal homologous recombination causes expansion and contraction of the repeats. In Huntington's disease, expansions over 30 repeats are considered pathogenic and induce aggregation of Huntington protein. *In vivo,* these aggregates form foci in the cell that under static imaging cannot be distinguished from liquid phase-separated condensates. The function of hydrotropes in biology is recently coming into appreciation and regulates the reversible formation of protein

Peer-reviewed version available at *Int. J. Mol. Sci.* **2020**, *21*, 1894; doi:10.3390/ijms21051894

condensates. Several proteins in the Mediator complex have IDRs that promote liquid phase-separated condensates with TFs [20]. Intrinsically disordered regions such a polyQ tracts facilitate phase separation [8,10–12,20,53]. The two polyQ tracts in Med15 vary between 12 and 27 repeats. Changes in polyQ tracts of Med15 changed the response to numerous chemicals and were dependent on Snf1. Throughout the tail proteins of the Meditator, there is genetic variation that has yet to be explored. Reciprocal hemizygosity of *med15* mutants did not differentiate between the YJM789 or BY4741 alleles. Both hemizygous mutants were more sensitive to MCHM than the homozygous mutant, despite the YJM789 strain having a higher tolerance to MCHM than BY4741. This was the case when Med15 was Myc tagged. Allele swapping of Med15^{YJM789} into BY4741 background conferred MCHM sensitivity but only in YPD and when the Myc tag was present. While in YJM789, the expression of Med15^{S288c}-Myc did not change MCHM resistance. In both BY4741 and YJM789 strains, the *med15* mutants were slow-growing in untreated media, which was not affected at higher concentrations of MCHM, making it appear that at the highest concentrations of MCHM, the YJM789 *med15* mutants were resistant to MCHM. MCHM sensitivity induced by expression of Med15^{YJM789} in BY4741 was not dominant. Therefore, we concluded that the YJM789 Mediator complex can better tolerate Med15 with shorter polyQ tracts, while the BY4741 Mediator is more sensitive to perturbations. Myc possibly increases recruitment of Snf1 to the Mediator when Med15 contains expanded polyQ tracts. *MED15*^{YJM789} was expressed at slightly lower levels and the protein level was even lower level than Med15^{S288c} and was also less stable. While changes in mRNA levels contribute to lower protein levels, the longer polyQ tracts in Med15^{YJM789} may also slow translation or increase ubiquitin-dependent degradation, as the protein is less stable when the translation was inhibited.

Ydj1 was required for stability of Med15 protein and it was difficult to assess the role of Ydj1 on Med15 protein stability because of the extremely slow growth of the *ydj1* mutants. Ydj1 also has a role at H3 histone eviction when transcription is induced. Gcn4 binding to promoters was not reduced in a *yjd1* mutant (Qiu *et al.* 2016) or at the *GAL1* promoter (Summers *et al.* 2009). Hsp70 associates with several Hsp40-like proteins including Ydj1, a type 1 Hsp40 that stimulates Hsp70 activity. Ydj1 is localized to the perinuclear and nuclear membranes (Caplan and Douglas 1991). The role in nucleosome eviction may be indirect by helping to fold Med15. Ydj1 inhibits the SDS-resistant aggregation of the polyQ containing a fragment of Htt in yeast (Krobitsch and Lindquist 1999; Muchowski *et al.* 2000). The Med15 fragment containing the polyQ aggregates *in vivo* (Zhu *et al.* 2015) as well as when full-length Med15 is overexpressed. Ydj1 was required for both alleles of Med15 protein stability as the isomers that were Myc tagged became less distinct maintaining Med15^{YJM789} true to size compared to Med15^{S288c}. Zinc can aid in catalysis as an enzyme cofactor but also stabilize the structure of proteins when bound and Ydj1 binds zinc. In response to zinc starvation, yeast ration their zinc, known as zinc sparing [57]. Intracellular zinc levels are three times higher when treated with MCHM, and supplementation with zinc improves growth up to a point when too much zinc can no longer rescue MCHM induced growth arrest [29]. Ydj1 protein level is dependent on zinc levels, although transcription was not affected [57]. For Ydj1, zinc may serve to stabilize the protein structure, protecting it from degradation as it unfolds without zinc. Yjd1 may function to regulate the phase state of Med15 or other components of the Mediator.

Yeast exposed to MCHM upregulate many pathways involved in biosynthesis; however, these yeast do not appear to be lacking for these nutrients. Amino acids, inositol, zinc, and phosphate levels are increased [29,30]. Since the 2014 MCHM spill, several studies have measured the

Peer-reviewed version available at *Int. J. Mol. Sci.* **2020**, *21*, 1894; doi:10.3390/ijms21051894

toxicological effects of MCHM on diverse species but have not addressed the mechanism of toxicity during acute exposure [58–65]. One possible explanation of MCHM's diverse effects is as a stable hydrotrope MCHM changes the structure of nutrient sensors so they no longer sense extracellular compounds. In YM, more genes were differentially expressed and yet yeast were more tolerant to MCHM. Compared to YPD, in YM, nutrient transporters are downregulated, and the biosynthetic pathways are upregulated which could mitigate the effect of MCHM. Familiar compounds such as ATP and RNA are hydrotropes and induce protein condensates which are separated from the surrounding proteins in liquid phase separation. This serves to concentrate functional proteins reversibly rather than inactivate them as protein aggregates. MCHM is a cyclic hydrocarbon that is relatively more stable than RNA and ATP in the cell. MCHM was detected in sediment ten months after the spill [65]. MCHM is primarily degraded into aldehydes and carboxylic acids [66] which generates ROS [67]. The increased ROS seen in this study was seen at 12 hours after incubation and therefore increase in ROS from degradation would be a secondary effect and the hydrotropic effect of MCHM would be the primary effect on the transcriptome and metabolome, especially at early time points.

Among the differentially expressed pathways in the *med15* mutant, *PHO89* was noted because Pho89 is a high-affinity transporter that is induced in inorganic phosphate limiting conditions [68] and intracellular levels of phosphate increase in MCHM exposure [29]. The other high-affinity inorganic phosphate transporter is Pho84, which is also induced in phosphate limiting conditions [69]. *PHO84* expression was 4-fold downregulated in the *med15* mutant grown in YPD but was not significantly different in other strains and conditions. While *PHO89* and *PHO84* are both induced in phosphate limiting conditions, the kinetics are slightly different due to the different transcription factors and kinases that regulate their expression [70]. Pho2/ Pho4 are transcription factors that regulate the PHO regulon and the expression of secreted acid phosphatases, Pho5, Pho11, and Pho12 was also increased in MCHM treatment. Yet there are other signaling pathways that affect the regulation of *PHO89,* such as Snf1, which phosphorylates Mig1 and Nrg1 under stress and regulate *PHO89* expression but not *PHO84* expression [70]. Pho84 and Pho89 have nonredundant roles in MCHM response. Despite *PHO89* being differentially expressed, only the *pho84* mutant was MCHM sensitive. It is likely that Med15 directly regulated *PHO84* expression because it physically binds the *PHO84* promoter, and it is not found at the *PHO89* promoter (B. Dunn, J. Gallagher, and M. Snyder, unpublished).

The multiple bands of Med15 proteins shift between the different alleles. In order to visualize Med15, the 13xMyc tag was integrated at the C-terminal end. While possible that the multiple bands represent N-terminal degradation products, most of these bands migrate slower than the predicted size of full-length Med15-Myc. Several lines of evidence pointed us to investigate whether Snf1 regulates Med15. Snf1 has been copurified with the Mediator complex [33]. Med15 has several phosphorylations in the C-terminal MAD. The *snf1* mutant is MCHM sensitive (Ayers *et al.,* in preparation) and Snf1 has a role in regulating *PHO89* [70]. In the *snf1* knockout, the impact of changes in the polyQ tract was only seen when Med15 was Myc tagged in MCHM treatment. In calcofluor white, caffeine, DTT, and hygromycin treatments, loss of Snf1 flipped the response of strains carrying untagged alleles of Med15. $Med15^{S288c}$ grew better than yeast with $Med15^{YJM789}$ in these stresses while yeast with $Med15^{YJM789}$ and *snf1* were more resistant in hydrogen peroxide. In western blots, the pattern of Med15 bands did not change in *snf1* knockout but did in the *reg1* knockout. Snf1 can be overactivated by knocking out Reg1, the repressor of SNF1. We did not address the nature of the different bands but they are

Peer-reviewed version available at *Int. J. Mol. Sci.* **2020**, *21*, 1894; doi:10.3390/ijms21051894

different from N-terminally tagged HA-Med15 [71], which looked more like the band patterns of Med15^{YJM789} but ran true to size compared to Med15^{YJM789}. Other studies have used Med15^{BY}-Myc for western blots, but the studies cropped the western blots so the pattern of bands could not be compared. However, Med15-Myc decreased the association of the rest of the Mediator tail subunits [72]. This leads to the hypothesis that a Myc tag on any component of the tail weakens the interaction with the rest of the complex [45]. However, a decreased association of Med15-Myc with the Mediator complex does not explain all the results presented here. Yeast with Med15^{YJM789}-Myc in BY4741 and hemizygous knockouts were more sensitive than *med15* knockouts to MCHM. If the stoichiometry of the Mediator was the only contributing factor to differences, then the phenotypes of the knockouts should show a more extreme version of hypomorphic alleles. This was directly tested by direct comparisons of growth between strains with different Med15 alleles with and without Myc tagged in diverse chemicals. The Myc tag can serve as an *in vitro* target of SNF1 (M. Schmidt, personal communication) and so if SNF1 is already associated with the Mediator, then the Myc tag may increase the SNF1-dependent phosphorylation of the Mediator.

The differences between Med15 alleles could only be seen in MCHM when Med15 was Myc tagged, while the impact of the tag sometimes exaggerated or lessened differences in other stresses, and sometimes had no impact. The original Myc tag was derived from a peptide from human c-Myc [73]. Myc is a family of oncogenic transcription factors. Of the multiple peptides tested, only 9E10 did not cross-react with c-myc from other organisms and had low background on western blots [73]. The 13xMyc epitope tag used here is tandem repeats of EQKLISEEDL [74]. Tagging a protein can affect folding, localization, and association with other proteins in a complex. Under normal conditions, Med2, Med3, and Med15 can be recruited to chromatin independent of the rest of the Mediator complex [72,75,76]. From the recent structures of the Mediator, Med2 and Med3 bind the C-terminal tail of Med14 in the body and directly bind Med15. Med15, in turn, binds Med16 and Med5 is at the very distal end of the tail (Figure 1A, [2]). The Med15-Med5-Med16 complex is posited to have a function independent of the full Mediator complex [46]. The Myc tag does not include the basic helix turn domain common in transcription factors that binds DNA. Other TFs regulated by the mediator such as Pho4 share homology with the DNA-binding domains of Myc proteins [38].

Conclusion

By their nature, the structure of intrinsically disordered regions are difficult to determine and are important for changes in protein complex conformations [20,23,77–79]. The fuzzy/ IDR domains of Med15 and the expansions of the polyQ tracts increased phenotypic diversity. Rim101, a transcription factor with a polyQ tract, affects allele-specific expression in one strain background but not others tested (Read *et al.* 2016). There are multiple phosphorylations in Med15 that regulate the transcriptional response to stress [35]. Expression of the longer Med15 allele changed the response to MCHM as other polymorphic transcription factors change the response to other chemical stressors [39]. Variation in key regulators permits the expression of cryptic genetic variation to alter phenotypes. These proteins are master variators.

Materials and Methods

Strain construction and cloning

All strains and sources are in Table S2. Med15 sequences were extracted from the sequenced genomes of BY4741, BY4742, AWRI1631, RM11-1a, and YJM789 (Song *et al.* 2015). Med15

Peer-reviewed version available at *Int. J. Mol. Sci.* **2020**, *21*, 1894; doi:10.3390/ijms21051894

was tagged at the C-terminus with a 13xMyc tag with KanR as the selectable marker in S288c (GSY147), BY4741, and YJM789 as previously described [39,74]. *MED15* has a polymorphism just after to the stop codon, so allele-specific primers were used for the 3' Myc tagging and knocking out (Table S3) Primers to the genomic *MED15* amplified 499 nucleotides upstream from the start and a 3' tagging primer to include the promoter, coding region, Myc tag, and KanR marker. The PCR product was then cloned into the NotI restriction site in pRS316. *MED15* was knocked out in YJM789K5a (isogenic with YJM789 except as a MATa prototroph) and then backcrossed to generate YJM789K6alpha as previously described (Rong-Mullins *et al.* 2017). The KanR marker of BY4741 knockout yeast of *snf1, reg1,* and *ydj1* (Giaever *et al.* 2002) was switched with HygR and then crossed with BY4742 *med15::NatR* to generate double mutants and then transformed with plasmids containing different alleles of *MED15.*

Because of the lack of convenient restriction sites and the repetitive nature, *MED15* domain swaps of the alleles proved challenging. Med15 domain swaps were carried out by PCR and then gap repair transformation of plasmid encoding $MED15^{YJM789}$ *-Myc* with polyQ inserts from $MED15^{S288c}$*.* We used inverted PCR to amply $pMED15^{YJM789}$*-Myc* plasmid to linearize the vector with gaps at each of the polyQ repeats. Each polyQ tract from $MED15^{S288c}$ was independently amplified with between 20 and 180 nucleotides of homology with the PCR amplified vector. The vector lacking polyQI and polyQII, respectively from the $pMED15^{YJM789}$*-Myc* plasmid was amplified using primers that generate between 20 and 180 nucleotides overlap at the 5' and 3' ends with the insert. and transformed with PCR amplified vector lacking polyQII. Cloning was carried out via gap repair transformation [84]. The inserts were amplified separately with flanking homology to the region around the vector's 5' and 3' ends. The insert and linear vector were transformed into BY4741 *med15* yeast and transformants were selected on YPD with G418. based on colony size, as *med15* yeast are slow-growing, in combination with selecting for markers on the plasmid. Genomic DNA was extracted and transformed into DH10 beta *E. coli* and then retransformed into BY4741 *med15.* All plasmids were verified by Sanger sequencing. Plasmids were rescued by passaging through *E. coli* and inserts were verified. All primers are listed in Table ST3.

Growth Conditions

Plasmids were maintained with the addition of 0.5 mg/ml G418 in YPD. In minimal media (YM), plasmids were maintained by supplementing media with uracil, histidine, and methionine, or by switching the nitrogen source to glutamate (MSG), and then adding G418 with amino acids as needed. Yeast were grown in liquid media as indicated to mid-log phase and then 550 ppm MCHM was added to YPD (650 ppm was added to YM) and cells were harvested after 30 minutes of exposure. Western blots were carried out as previously described (Gallagher *et al.* 2014). Solid media plates were cooled to 65ºC before MCHM was added and gently mixed until dissolved. Plates were used within 24 hours to limit the evaporation of MCHM. Yeast were serially diluted 10-fold and spotted on to solid media. Plates were photographed after 2-3 days of growth. For multiple drug screening in the TECAN, the automated plate reader, yeast were grown to stationary phase and then diluted to 0.1 OD with appropriate drugs and read at OD_{600} (Rong-Mullins *et al.* 2017). The following chemicals were added: 3mM hydrogen peroxide (H_20_2), 0.25 μg/ ml 4-Nitroquinoline 1-oxide (4NQO), 400 ppm 4-Methylcyclohexanol (MCHM), 1 mM copper sulfate ($CuSO_4$), 7.5 ng/ml rapamycin (Rapa), 0.1% glyphosate (CR41), 100 mM hydroxyurea (HU), 20 μg/ml camptothecin (CPT), 8.5 mM beta-mercaptoethanol (βME), 5 mM calcofluor white (CALC), 2.5 mM caffeine (CAFF), 20 mM Dithiothreitol (DTT), and 50 μg/ ml

Peer-reviewed version available at *Int. J. Mol. Sci.* **2020**, *21*, 1894; doi:10.3390/ijms21051894

hygromycin. Cells were grown with readings taken every hour. During log-phase, the OD_{600} of yeast carrying *MED15*^{S288c} was subtracted from *MED15*^{YJM789} at the point of maximal growth difference.

Transcriptomics

RNAseq was carried out in biological triplicate from yeast grown in YM supplemented with histidine, leucine, and methionine or YPD with G418. PolyA RNA was selected using Karpa Stranded RNAseq library preparation kit according to the manufacturer's instructions (catalog number KK8401). Libraries were sequenced on Illumina PE50bp high output flowcell. Basecalls were performed with Illumina's FASTQ Generation (v1.0.0) available in BaseSpace. Transcripts quantification was done with salmon (v0.9.1) vs the transcripts file BY4741_Toronto_2012_cds.fsa (available from https://downloads.yeastgenome.org/sequence/strains/BY4741/BY4741_Toronto_2012/). This data is available from GSE, accession number GSE129898 (https://www.ncbi.nlm.nih.gov/geo/query/acc.cgi?acc=GSE129898). Quantification tables were imported to R (3.4.4) and gene-level analysis was created with the tximport (1.6.0) package. For the transcripts to gene translation the homemade R package TxDb.Scerevisiae.SGD.BY4741 was used. This package was built from the BY4741_Toronto_2012.gff file using GenomicFeatures (1.30.3). The gene differential expression analysis and the data quality assessment were done with DESeq2 (1.18.1). p values were adjusted to an FDR of 0.005. The MA-plots were done with ggpubr (0.1.6).

GO term analysis was carried out with clusterProfiler [85] (3.6.0). The ORF names from genes up or downregulated in each condition were translated to the correspondent Entrez id using the function bitr and the package org.Sc.sgd.db. The resulting gene clusters were processed with the compareCluster function, in mode enrichGO, using org.Sc.sgd.db as a database, with Biological Process ontology, cutoffs of p-value = 0.01 and q value = 0.05, adjusted by FDR , to generate the corresponding GO profiles, which were then simplified with the function simplify. The simplified profiles were represented as dotplots, showing up to 15 more relevant categories.

Western blot

Proteins were extracted, immunoprecipitated, separated in 5-12% SDS-PAGE, and transferred onto 0.2 micron PVDF as previously described [39]. Antibodies were diluted into freshly made 3% BSA Fraction V in TBS-Tween. ECL kit and HRP secondary antibodies were used to visualize mouse anti-Myc E910 (1:7,500) from various manufacturers and rabbit anti-PGK (1:10,000) on a Protein Simple using default chemiluminescence setting.

Flow cytometry

BY4741 cells were grown to saturation overnight and returned to mid-log phase. Cells were then diluted to a starting OD_{600} of 0.3 in biological triplicate in YPD media containing MCHM. For measurement of ROS, live cells were pelleted then suspended in 200µl of 50mM DHE in phosphate-buffered saline (PBS). The dyed cultures were incubated at 30ºC for 20 minutes and washed with PBS. A positive control sample of BY4741 cells were treated with 25mM H_2O_2 for 1.5 hours. The DHE dyed samples were then analyzed within 2 hours of harvesting on a BD LSRFortessa using preset propidium iodide detection defaults. Approximately 30,000 events were collected per sample for downstream analysis.

Peer-reviewed version available at *Int. J. Mol. Sci.* **2020**, *21*, 1894; doi:10.3390/ijms21051894

Acknowledgments

Angela Lee generously gave us the yeast knockout collection. The Gallagher lab provided a fruitful discussion. We would like to acknowledge the WVU Genomics Core Facility, Morgantown, WV for the support provided to help make this publication possible including RNAseq library construction and sequencing. WVU Flow Cytometry & Single Cell Core Fortessa S10 instrument was supported by OD016165 and WV-INBRE grant 103434. The Pgk1 antibody was a gift from Jeremy Thorner at the University of California, Berkeley. This work was supported by a grant from the NIH NIES (R15ES026811-01A1).

Conflict of interest

The authors declare that they have no conflicts of interest with the contents of this article.

Author contributions

Concepulation, JEGG; Investigation, JEGG; Writing – Orginial Draft Preparation, JEGG; Writing – Review & Editing, JEGG, SLS, MCA, and NC; Visulation, JEGG and AP; Supervision, JEGG; and Fuding Acquistion, JEGG.

Supplemental Figure and Table Legends

Figure S1 (A) Reciprocal hemizygotes of Med15 in BY4741xYJM789 hybrids were grown on MCHM in YPD. Med15 was tagged at the chromosomal locus with 13xMyc at the C-terminal end or knockout with a dominant drug marker in haploid parents. Yeast were then mated, and diploids selected. An equal number of yeast were serially diluted and plated onto YPD with the indicated amount of MCHM. (B**)** BY4741 yeast (wildtype) and BY4741 *med15::NatR* (*med15)* were transformed with pGS35 (empty) or pGS35-*MED15-Myc* (p*MED15*^{YJM789}Myc and p*MED15*^{S2889}Myc). Plasmids were maintained with G418 in YPD and YM with glutamate (MSG) as the nitrogen source. Yeast were serially diluted and plated with indicated amounts of MCHM.

Figure S2 GO term analysis on genes that are downregulated in *med15* mutants grown in YPD or YPD + 550 ppm MCHM compared to BY4741 and BY4741 expressing *MED15*^{YJM789} compared to BY4741 grown in YPD + 550 ppm MCHM.

Figure S3 GO term analysis on genes that are upregulated in *med15* mutants grown in YPD or YPD + 550 ppm MCHM compared to BY4741, and BY4741 expressing *MED15*^{YJM789} compared to BY4741 grown in YPD + 550 ppm MCHM.

Figure S4. Changes in the transcriptome of BY4741 yeast carrying different alleles of Med15 treated with MCHM grown in YM. (A) Differentially expressed mRNA from wildtype yeast (BY4741) compared to a *med15* knockout strain grown in YPD. (B) Differentially expressed mRNA from wildtype yeast (BY4741) compared to a *med15* knockout strain grown in YM then shifted to 550 ppm MCHM for 30 minutes. (C) Differentially expressed mRNA from wildtype yeast (BY4741) compared to a *med15* knockout strain carrying Med15^{YJM789} expressed from a plasmid grown in YM then shifted to 650 ppm MCHM for 30 minutes. (D) Differentially expressed mRNA from wildtype yeast (BY4741) compared to a *med15* knockout strain carrying Med15^{S288c} expressed from a plasmid grown in YM with G418 then shifted to 650 ppm MCHM for 30 minutes.

Figure S5 GO term analysis on genes that are downregulated in *med15* mutants grown in YM or YM + 650 ppm MCHM compared to BY4741.

Peer-reviewed version available at *Int. J. Mol. Sci.* **2020**, *21*, 1894; doi:10.3390/ijms21051894

Figure S6 GO term analysis on genes that are upregulated in *med15* mutants grown in YM or YM + 650 ppm MCHM compared to BY4741, and BY4741 expressing $MED15^{YJM789}$-Myc compared to BY4741 grown in YM + MCHM.

Figure S7 Impact of hydrogen peroxide and MCHM on Med15 and Reactive Oxygen Species levels. (A) Western blot of Med15-Myc immunoprecipitated from BY4741 grown in YPD at 0, 10, 20, 40, 60 and 90 minutes after the addition of 550 ppm MCHM or H_2O_2. (B) Levels of ROS in strains of yeast exposed to MCHM, based on fluorescence of the ROS-reactive dye DHE. Yeast were incubated for 12 hours with or without MCHM then stained with DHE for 20 minutes before cells were sorted using flow cytometry. Hydrogen peroxide treatment for 1.5 hours was used as a positive control to generate ROS in wildtype (WT, BY4741) (black line) and *med15* knockout yeast (grey line). Background ROS of untreated yeast in dark blue measures endogenous ROS compared *med15* in light blue. MCHM WT yeast are in red while MCHM treated m*ed15* yeast in orange. The y-axis represents the number of cells and the x-axis represents the fluorescence of DHE conversion to ethidium bromide by ROS.

Figure S8. Changes in the transcriptome of BY4741 or yeast carrying or $Med15^{BY}$ $Med15^{S288c}$-Myc. (A) Differentially expressed mRNA from wildtype yeast (BY4741) compared to a *med15* knockout with $Med15^{S288c}$-13xMyc strain grown in YPD. (B) Differentially expressed mRNA from wildtype yeast (BY4741) compared to a *med15* knockout with $Med15^{S288c}$-Myc strain grown in YPD. (C) Serial dilution of BY4741 with $Med15^{BY}$ or $Med15^{S288c}$ with and without the Myc tag.

Table S1 Differentially Expressed Gene list from BY4741, BY4741 *med15::NAT* (BYmed15), BY4741 *med15::NAT* with $pMed15^{YJM789}$-Myc (BYpMM_789), and BY4741 *med15::NAT* with $pMed15^{S288c}$-Myc (BYpMM_S288c) grown in YPD or YM with or without 550 ppm MCHM.

Table S2 Strain list.

Table S3 Primer list. All primers are listed 5' to 3' and the relative direction to *MED15* is noted in the name. +/- notes the distance of the primer from the 5' end of $MED15^{S288c}$ or the junction of the genomic integration of the tag or the knockout cassette.

References

1. Verger, A.; Monté, D.; Villeret, V. Twenty years of Mediator complex structural studies. *Biochem. Soc. Trans.* **2019**, *47*, 399–410.

2. Robinson, P.J.; Trnka, M.J.; Pellarin, R.; Greenberg, C.H.; Bushnell, D.A.; Davis, R.; Burlingame, A.L.; Sali, A.; Kornberg, R.D. Molecular architecture of the yeast Mediator complex. *Elife* **2015**, *4*, e08719.

3. Tsai, K.L.; Tomomori-Sato, C.; Sato, S.; Conaway, R.C.; Conaway, J.W.; Asturias, F.J. Subunit architecture and functional modular rearrangements of the transcriptional mediator complex. *Cell* **2014**, *157*, 1430–1444.

4. Tsai, K.-L.; Yu, X.; Gopalan, S.; Chao, T.-C.; Zhang, Y.; Florens, L.; Washburn, M.P.; Murakami, K.; Conaway, R.C.; Conaway, J.W.; et al. Mediator structure and rearrangements required for holoenzyme formation. *Nature* **2017**, *544*, 196–201.

5. Bourbon, H.-M. Comparative genomics supports a deep evolutionary origin for the large, four-module transcriptional mediator complex. *Nucleic Acids Res.* **2008**, *36*, 3993–4008.

6. Cooper, D.G.; Fassler, J.S. Med15: Glutamine-Rich Mediator Subunit with Potential for

Peer-reviewed version available at *Int. J. Mol. Sci.* **2020**, *21*, 1894; doi:10.3390/ijms21051894

Plasticity. *Trends Biochem. Sci.* **2019**.

7. Michelitsch, M.D.; Weissman, J.S. A census of glutamine/asparagine-rich regions: Implications for their conserved function and the prediction of novel prions. *Proc. Natl. Acad. Sci. U. S. A.* **2000**, *97*, 11910–11915.

8. Tuttle, L.M.; Pacheco, D.; Warfield, L.; Luo, J.; Ranish, J.; Hahn, S.; Klevit, R.E. Gcn4-Mediator Specificity Is Mediated by a Large and Dynamic Fuzzy Protein-Protein Complex. *Cell Rep.* **2018**, *22*, 3251–3264.

9. Pacheco, D.; Warfield, L.; Brajcich, M.; Robbins, H.; Luo, J.; Ranish, J.; Hahn, S. Transcription Activation Domains of the Yeast Factors Met4 and Ino2: Tandem Activation Domains with Properties Similar to the Yeast Gcn4 Activator. *Mol. Cell. Biol.* **2018**, *38*, e00038-18.

10. Warfield, L.; Tuttle, L.M.; Pacheco, D.; Klevit, R.E.; Hahn, S. A sequence-specific transcription activator motif and powerful synthetic variants that bind Mediator using a fuzzy protein interface. *Proc Natl Acad Sci U S A* **2014**, *111*, E3506-13.

11. Brzovic, P.S.; Heikaus, C.C.; Kisselev, L.; Vernon, R.; Herbig, E.; Pacheco, D.; Warfield, L.; Littlefield, P.; Baker, D.; Klevit, R.E.; et al. The acidic transcription activator Gcn4 binds the mediator subunit Gal11/Med15 using a simple protein interface forming a fuzzy complex. *Mol Cell* **2011**, *44*, 942–953.

12. Jedidi, I.; Zhang, F.; Qiu, H.; Stahl, S.J.; Palmer, I.; Kaufman, J.D.; Nadaud, P.S.; Mukherjee, S.; Wingfield, P.T.; Jaroniec, C.P.; et al. Activator Gcn4 employs multiple segments of Med15/Gal11, including the KIX domain, to recruit mediator to target genes in vivo. *J Biol Chem* **2010**, *285*, 2438–2455.

13. Zhu, X.; Chen, L.; Carlsten, J.O.P.; Liu, Q.; Yang, J.; Liu, B.; Gustafsson, C.M. Mediator tail subunits can form amyloid-like aggregates in vivo and affect stress response in yeast. *Nucleic Acids Res.* **2015**, *43*, 7306–14.

14. Baxendale, S.; MacDonald, M.E.; Mott, R.; Francis, F.; Lin, C.; Kirby, S.F.; James, M.; Zehetner, G.; Hummerich, H.; Valdes, J. A cosmid contig and high resolution restriction map of the 2 megabase region containing the Huntington's disease gene. *Nat Genet* **1993**, *4*, 181–186.

15. Landles, C.; Bates, G.P. Huntingtin and the molecular pathogenesis of Huntington's disease. *EMBO Rep.* **2004**, *5*, 958–963.

16. Krobitsch, S.; Lindquist, S. Aggregation of huntingtin in yeast varies with the length of the polyglutamine expansion and the expression of chaperone proteins. *Proc. Natl. Acad. Sci.* **1999**, *97*, 1589–1594.

17. Gillies, A.T.; Taylor, R.; Gestwicki, J.E. Synthetic lethal interactions in yeast reveal functional roles of J protein co-chaperones. *Mol. Biosyst.* **2012**, *8*, 2901–8.

18. Hines, J.K.; Li, X.; Du, Z.; Higurashi, T.; Li, L.; Craig, E.A. [SWI], the prion formed by the chromatin remodeling factor Swi1, is highly sensitive to alterations in Hsp70 chaperone system activity. *PLoS Genet.* **2011**, *7*, e1001309.

19. Alberti, S.; Halfmann, R.; King, O.; Kapila, A.; Lindquist, S. A systematic survey identifies prions and illuminates sequence features of prionogenic proteins. *Cell* **2009**, *137*, 146–158.

Peer-reviewed version available at *Int. J. Mol. Sci.* **2020**, *21*, 1894; doi:10.3390/ijms21051894

20. Boija, A.; Klein, I.A.; Sabari, B.R.; Dall'Agnese, A.; Coffey, E.L.; Zamudio, A. V.; Li, C.H.; Shrinivas, K.; Manteiga, J.C.; Hannett, N.M.; et al. Transcription Factors Activate Genes through the Phase-Separation Capacity of Their Activation Domains. *Cell* **2018**, *175*, 1842-1855.e16.

21. Hahn, S. Phase Separation, Protein Disorder, and Enhancer Function. *Cell* **2018**, *175*, 1723–1725.

22. Alberti, S.; Gladfelter, A.; Mittag, T. Considerations and Challenges in Studying Liquid-Liquid Phase Separation and Biomolecular Condensates. *Cell* **2019**, *176*, 419–434.

23. Patel, A.; Malinovska, L.; Saha, S.; Wang, J.; Alberti, S.; Krishnan, Y.; Hyman, A.A. ATP as a biological hydrotrope. *Science (80-.).* **2017**, *356*, 753–756.

24. Hayes, M.H.; Peuchen, E.H.; Dovichi, N.J.; Weeks, D.L. Dual roles for ATP in the regulation of phase separated protein aggregates in Xenopus oocyte nucleoli. *Elife* **2018**, *7*, e35224.

25. Kang, J.; Lim, L.; Song, J. ATP enhances at low concentrations but dissolves at high concentrations liquid-liquid phase separation (LLPS) of ALS/FTD-causing FUS. *Biochem. Biophys. Res. Commun.* **2018**, *504*, 545–551.

26. Lin, Y.; Protter, D.S.W.; Rosen, M.K.; Parker, R. Formation and Maturation of Phase-Separated Liquid Droplets by RNA-Binding Proteins. *Mol. Cell* **2015**, *60*, 208–19.

27. Hsu, J.; Del Rosario, M.C.; Thomasson, E.; Bixler, D.; Haddy, L.; Duncan, M.A. Hospital Impact after a Chemical Spill That Compromised the Potable Water Supply: West Virginia, January 2014. *Disaster Med. Public Health Prep.* **2017**, *11*, 621–624.

28. Thomasson, E.D.; Scharman, E.; Fechter-Leggett, E.; Bixler, D.; Ibrahim, S.; Duncan, M.A.; Hsu, J.; Scott, M.; Wilson, S.; Haddy, L.; et al. Acute health effects after the Elk River chemical spill, West Virginia, January 2014. *Public Health Rep.* **2017**, *132*, 196–202.

29. Pupo, A.; Ayers, M.C.; Sherman, Z.N.; Vance, R.J.; Cumming, J.R.; Gallagher, J.E.G.G. MCHM Acts as a Hydrotrope, Altering the Balance of Metals in Yeast. *Biol. Trace Elem. Res.* **2019**, 1–12.

30. Pupo, A.; Ku, K.M.; Gallagher, J.E.G. Effects of MCHM on yeast metabolism. *PLoS One* **2019**, *14*.

31. Hedbacker, K.; Carlson, M. SNF1/AMPK pathways in yeast. *Front. Biosci.* 2008, *13*, 2408–2420.

32. Simpson-Lavy, K.; Kupiec, M. A reversible liquid drop aggregation controls glucose response in yeast. *Curr. Genet.* 2018, *64*, 785–788.

33. Uthe, H.; Vanselow, J.T.; Schlosser, A. Proteomic Analysis of the Mediator Complex Interactome in Saccharomyces cerevisiae. *Sci. Rep.* **2017**, *7*.

34. Poss, Z.C.; Ebmeier, C.C.; Taatjes, D.J. The Mediator complex and transcription regulation. *Crit. Rev. Biochem. Mol. Biol.* **2013**, *48*, 575–608.

35. Miller, C.; Matic, I.; Maier, K.C.; Schwalb, B.; Roether, S.; Strasser, K.; Tresch, A.; Mann, M.; Cramer, P. Mediator phosphorylation prevents stress response transcription during non-stress conditions. *J Biol Chem* **2012**, *287*, 44017–44026.

Peer-reviewed version available at *Int. J. Mol. Sci.* **2020**, *21*, 1894; doi:10.3390/ijms21051894

36. Korber, P.; Barbaric, S. The yeast PHO5 promoter: From single locus to systems biology of a paradigm for gene regulation through chromatin. *Nucleic Acids Res.* 2014, *42*, 10888–10902.

37. Shao, D.; Creasy, C.L.; Bergman, L.W. *A cysteine residue in helix II of the bHLH domain is essential for homodimerization of the yeast transcription factor Pho4p*; 1998; Vol. 26;.

38. Shao, D.; Creasy, C.L.; Bergman, L.W. Interaction of Saccharomyces cerevisiae Pho2 with Pho4 increases the accessibility of the activation domain of Pho4. *Mol. Gen. Genet.* **1996**, *251*, 358–64.

39. Gallagher, J.E.G.; Zheng, W.; Rong, X.; Miranda, N.; Lin, Z.; Dunn, B.; Zhao, H.; Snyder, M.P. Divergence in a master variator generates distinct phenotypes and transcriptional responses. *Genes Dev* **2014**, *28*, 409–421.

40. Rong-Mullins, X.X.; Ayers, M.C.; Summers, M.; Gallagher, J.E.G. Transcriptional Profiling of Saccharomyces cerevisiae Reveals the Impact of Variation of a Single Transcription Factor on Differential Gene Expression in 4NQO, Fermentable, and Nonfermentable Carbon Sources. *G3 Genes, Genomes, Genet.* **2018**, *8*.

41. Swaney, D.L.; Beltrao, P.; Starita, L.; Guo, A.; Rush, J.; Fields, S.; Krogan, N.J.; Villén, J.; Villen, J. Global analysis of phosphorylation and ubiquitylation cross-talk in protein degradation. *Nat Methods* **2013**, *10*, 676–682.

42. Albuquerque, C.P.; Smolka, M.B.; Payne, S.H.; Bafna, V.; Eng, J.; Zhou, H. A multidimensional chromatography technology for in-depth phosphoproteome analysis. *Mol. Cell. Proteomics* **2008**, *7*, 1389–96.

43. Holt, L.J.; Tuch, B.B.; Villén, J.; Johnson, A.D.; Gygi, S.P.; Morgan, D.O. Global analysis of Cdk1 substrate phosphorylation sites provides insights into evolution. *Science* **2009**, *325*, 1682–6.

44. Soulard, A.; Cremonesi, A.; Moes, S.; Schütz, F.; Jenö, P.; Hall, M.N. The Rapamycin-sensitive Phosphoproteome Reveals That TOR Controls Protein Kinase A Toward Some But Not All Substrates. *Mol. Biol. Cell* **2010**, *21*, 3475–3486.

45. Ansari, S.A.; Ganapathi, M.; Benschop, J.J.; Holstege, F.C.P.; Wade, J.T.; Morse, R.H. Distinct role of Mediator tail module in regulation of SAGA-dependent, TATA-containing genes in yeast. *EMBO J.* **2011**, *31*, 44–57.

46. Larsson, M.; Uvell, H.; Sandstrom, J.; Ryden, P.; Selth, L.A.; Bjorklund, S. Functional studies of the yeast med5, med15 and med16 mediator tail subunits. *PLoS One* **2013**, *8*, e73137.

47. Island, M.D.; Perry, J.R.; Naider, F.; Becker, J.M. Isolation and characterization of S. cerevisiae mutants deficient in amino acid-inducible peptide transport. *Curr. Genet.* **1991**, *20*, 457–463.

48. Vandenbol, M.; Jauniaux, J.C.; Grenson, M. Nucleotide sequence of the Saccharomyces cerevisiae PUT4 proline-permease-encoding gene: similarities between CAN1, HIP1 and PUT4 permeases. *Gene* **1989**, *83*, 153–159.

49. Mara, P.; Fragiadakis, G.S.; Gkountromichos, F.; Alexandraki, D. The pleiotropic effects of the glutamate dehydrogenase (GDH) pathway in Saccharomyces cerevisiae. *Microb. Cell Fact.* **2018**, *17*, 170.

Peer-reviewed version available at *Int. J. Mol. Sci.* **2020**, *21*, 1894; doi:10.3390/ijms21051894

50. Villers, J.; Savocco, J.; Szopinska, A.; Degand, H.; Nootens, S.; Morsomme, P. Study of the Plasma Membrane Proteome Dynamics Reveals Novel Targets of the Nitrogen Regulation in Yeast. *Mol. Cell. Proteomics* **2017**, *16*, 1652–1668.

51. Caplan, A.J.; Douglas, M.G. Characterization of YDJ1: a yeast homologue of the bacterial dnaJ protein. *J. Cell Biol.* **1991**, *114*, 609–21.

52. Gallagher, D.L.; Phetxumphou, K.; Smiley, E.; Dietrich, A.M. Tale of Two Isomers: Complexities of Human Odor Perception for *cis* - and *trans* -4-Methylcyclohexane Methanol from the Chemical Spill in West Virginia. *Environ. Sci. Technol.* **2015**, *49*, 1319–1327.

53. Hyman, A.A.; Weber, C.A.; Ulicher, F.J.¨ Downloaded from www.annualreviews.org Access provided by West Virginia University on 05/17/19. For personal use only. *Annu. Rev. Cell Dev. Biol* **2014**, *30*, 39–58.

54. Qiu, H.; Chereji, R. V; Hu, C.; Cole, H.A.; Rawal, Y.; Clark, D.J.; Hinnebusch, A.G. Genome-wide cooperation by HAT Gcn5, remodeler SWI/SNF, and chaperone Ydj1 in promoter nucleosome eviction and transcriptional activation. *Genome Res.* **2016**, *26*, 211–25.

55. Summers, D.W.; Douglas, P.M.; Ren, H.-Y.; Cyr, D.M. The type I Hsp40 Ydj1 utilizes a farnesyl moiety and zinc finger-like region to suppress prion toxicity. *J. Biol. Chem.* **2009**, *284*, 3628–39.

56. Muchowski, P.J.; Schaffar, G.; Sittler, A.; Wanker, E.E.; Hayer-Hartl, M.K.; Hartl, F.U. Hsp70 and hsp40 chaperones can inhibit self-assembly of polyglutamine proteins into amyloid-like fibrils. *Proc. Natl. Acad. Sci. U. S. A.* **2000**, *97*, 7841–6.

57. Wang, Y.; Weisenhorn, E.; MacDiarmid, C.W.; Andreini, C.; Bucci, M.; Taggart, J.; Banci, L.; Russell, J.; Coon, J.J.; Eide, D.J. The cellular economy of the *Saccharomyces cerevisiae* zinc proteome. *Metallomics* **2018**, *10*, 1755–1776.

58. Eastman, C. Eastman Crude MCHM Studies Available online: http://www.eastman.com/Pages/Eastman-Crude-MCHM-Studies.aspx.

59. Horzmann, K.A.; de Perre, C.; Lee, L.S.; Whelton, A.J.; Freeman, J.L. Comparative analytical and toxicological assessment of methylcyclohexanemethanol (MCHM) mixtures associated with the Elk River chemical spill. *Chemosphere* **2017**, *188*, 599–607.

60. Han, A.A.; Fabyanic, E.B.; Miller, J. V.; Prediger, M.S.; Prince, N.; Mouch, J.A.; Boyd, J. In vitro cytotoxicity assessment of a West Virginia chemical spill mixture involving 4-methylcyclohexanemethanol and propylene glycol phenyl ether. *Environ. Monit. Assess.* **2017**, *189*, 190.

61. Phetxumphou, K.; Dietrich, A.M.; Shanaiah, N.; Smiley, E.; Gallagher, D.L. Subtleties of human exposure and response to chemical mixtures from spills. *Environ. Pollut.* **2016**, *214*, 618–626.

62. Gwinn, W.M.; Bousquet, R.W.; Perry, C.E.; Urbano, N.C.; Auerbach, S.S. *NTP Research Report on the Preliminary Evaluation of 4-Methylcyclohexylmethanol in an In Vitro Human Airway Model*; National Toxicology Program, 2018;

63. Weidhaas, J.; Lin, L.-S.; Buzby, K.; Li, X. Biodegradation of MCHM and PPH in River Microcosms and Activated Sludge. *J. Environ. Eng.* **2016**, *142*, 04016056.

Peer-reviewed version available at *Int. J. Mol. Sci.* **2020**, *21*, 1894; doi:10.3390/ijms21051894

64. Paustenbach, D.J.; Winans, B.; Novick, R.M.; Green, S.M. The toxicity of crude 4-methylcyclohexanemethanol (MCHM): review of experimental data and results of predictive models for its constituents and a putative metabolite. *Crit. Rev. Toxicol.* **2015**, *45*, 1–55.

65. Cozzarelli, I.M.; Akob, D.M.; Baedecker, M.J.; Spencer, T.; Jaeschke, J.; Dunlap, D.S.; Mumford, A.C.; Poret-Peterson, A.T.; Chambers, D.B. Degradation of Crude 4-MCHM (4-Methylcyclohexanemethanol) in Sediments from Elk River, West Virginia. *Environ. Sci. Technol.* **2017**, *51*, 12139–12145.

66. Lan, J.; Hu, M.; Gao, C.; Alshawabkeh, A.; Gu, A.Z. Toxicity Assessment of 4-Methyl-1-cyclohexanemethanol and Its Metabolites in Response to a Recent Chemical Spill in West Virginia, USA. *Environ. Sci. Technol.* **2015**.

67. Cui, D.; Mebel, A.M.; Arroyo-Mora, L.E.; Holness, H.; Furton, K.G.; O'Shea, K. Kinetic, product, and computational studies of the ultrasonic induced degradation of 4-methylcyclohexanemethanol (MCHM). *Water Res.* **2017**, *126*, 164–171.

68. Martinez, P.; Persson, B.L. Identification, cloning and characterization of a derepressible Na+-coupled phosphate transporter in Saccharomyces cerevisiae. *Mol. Gen. Genet.* **1998**, *258*, 628–638.

69. Bun-Ya, M.; Nishimura, M.; Harashima, S.; Oshima, Y. The PHO84 gene of Saccharomyces cerevisiae encodes an inorganic phosphate transporter. *Mol. Cell. Biol.* **1991**, *11*, 3229–3238.

70. Serra-Cardona, A.; Petrezselyova, S.; Canadell, D.; Ramos, J.; Arino, J. Coregulated Expression of the Na+/Phosphate Pho89 Transporter and Ena1 Na+-ATPase Allows Their Functional Coupling under High-pH Stress. *Mol. Cell. Biol.* **2014**, *34*, 4420–4435.

71. Herbig, E.; Warfield, L.; Fish, L.; Fishburn, J.; Knutson, B.A.; Moorefield, B.; Pacheco, D.; Hahn, S. Mechanism of Mediator recruitment by tandem Gcn4 activation domains and three Gal11 activator-binding domains. *Mol Cell Biol* **2010**, *30*, 2376–2390.

72. Zhang, F.; Sumibcay, L.; Hinnebusch, A.G.; Swanson, M.J. A triad of subunits from the Gal11/tail domain of Srb mediator is an in vivo target of transcriptional activator Gcn4p. *Mol. Cell. Biol.* **2004**, *24*, 6871–86.

73. Evan, G.I.; Lewis, G.K.; Ramsay, G.; Bishop, J.M. Isolation of monoclonal antibodies specific for human c-myc proto-oncogene product. *Mol. Cell. Biol.* **1985**, *5*, 3610–3616.

74. Bähler, J.; Wu, J.-Q.; Longtine, M.S.; Shah, N.G.; Mckenzie III, A.; Steever, A.B.; Wach, A.; Philippsen, P.; Pringle, J.R. Heterologous modules for efficient and versatile PCR-based gene targeting inSchizosaccharomyces pombe. *Yeast* **1998**, *14*, 943–951.

75. Anandhakumar, J.; Moustafa, Y.W.; Chowdhary, S.; Kainth, A.S.; Gross, D.S. Evidence for Multiple Mediator Complexes in Yeast Independently Recruited by Activated Heat Shock Factor. *Mol. Cell. Biol.* **2016**, *36*, 1943–1960.

76. He, Q.; Battistella, L.; Morse, R.H. Mediator requirement downstream of chromatin remodeling during transcriptional activation of CHA1 in yeast. *J. Biol. Chem.* **2008**, *283*, 5276–5286.

77. Sabari, B.R.; Dall'Agnese, A.; Boija, A.; Klein, I.A.; Coffey, E.L.; Shrinivas, K.; Abraham, B.J.; Hannett, N.M.; Zamudio, A. V.; Manteiga, J.C.; et al. Coactivator condensation at super-enhancers links phase separation and gene control. *Science (80-.).* **2018**, *361*,

Peer-reviewed version available at *Int. J. Mol. Sci.* **2020**, *21*, 1894; doi:10.3390/ijms21051894

eaar3958.

78. Boehning, M.; Dugast-Darzacq, C.; Rankovic, M.; Hansen, A.S.; Yu, T.; Marie-Nelly, H.; McSwiggen, D.T.; Kokic, G.; Dailey, G.M.; Cramer, P.; et al. RNA polymerase II clustering through carboxy-terminal domain phase separation. *Nat. Struct. Mol. Biol.* **2018**, *25*, 833–840.

79. Cho, W.-K.; Spille, J.-H.; Hecht, M.; Lee, C.; Li, C.; Grube, V.; Cisse, I.I. Mediator and RNA polymerase II clusters associate in transcription-dependent condensates. *Science (80-.).* **2018**, *361*, 412–415.

80. Read, T.; Richmond, P.A.; Dowell, R.D.; Félix, M.; Bentley, D.; Chakravarti, A. A trans-acting Variant within the Transcription Factor RIM101 Interacts with Genetic Background to Determine its Regulatory Capacity. *PLOS Genet.* **2016**, *12*, e1005746.

81. Song, G.; Dickins, B.J.; Demeter, J.; Engel, S.; Gallagher, J.; Choe Barbara., K.D.; Cherry, J.M. AGAPE (Automated Genome Analysis PipelinE) for pan-genome analysis of Saccharomyces cerevisiae. *PLoS One* **2015**, *10*, e0120671.

82. Rong-Mullins, X.; Winans, M.J.J.; Lee, J.B.B.; Lonergan, Z.R.R.; Pilolli, V.A.A.; Weatherly, L.M.M.; Carmenzind, T.W.W.; Jiang, L.; Cumming, J.R.R.; Oporto, G.S.S.; et al. Proteomic and genetic analysis of S. cerevisiae response to soluble copper leads to improvement of antimicrobial function of cellulosic copper nanoparticles. *Metallomics* **2017**, *9*, 1304–1315.

83. Giaever, G.; Chu, A.M.; Ni, L.; Connelly, C.; Riles, L.; Veronneau, S.; Dow, S.; Lucau-Danila, A.; Anderson, K.; Andre, B.; et al. Functional profiling of the Saccharomyces cerevisiae genome. *Nature* **2002**, *418*, 387–391.

84. Gallagher, J.E.G.; Baserga, S.J. Two-hybrid Mpp10p interaction-defective Imp4 proteins are not interaction defective in vivo but do confer specific pre-rRNA processing defects in Saccharomyces cerevisiae. *Nucleic Acids Res.* **2004**, *32*, 1404–1413.

85. Yu, G.; Wang, L.-G.; Han, Y.; He, Q.-Y. clusterProfiler: an R Package for Comparing Biological Themes Among Gene Clusters. *Omi. A J. Integr. Biol.* **2012**, *16*, 284–287.